Long Term Variation of Mean Transit Time in Spring and Groundwater in a Forested Headwater Catchment

January 2023

Isabela Silveira Baptista

Long Term Variation of Mean Transit Time in Spring and Groundwater in a Forested Headwater Catchment

A Dissertation Submitted to

the Graduate School of Science and Technology,

University of Tsukuba

in Partial Fulfillment of Requirements

for the Degree of Doctor of Philosophy in Environmental Studies

Doctoral Program in Environmental Studies,

Degree Programs in Life and Earth Sciences

Isabela Silveira Baptista

How thinned forests change

the hidden groundwater time?

Tracers show the date!

-Winner poem written for the
AGU Water Quality
#HaikuYourResearch 2022 Competition

Abstract

In recent years, there have been studies aiming to understand the effect that thinning of plantation forests in Japanese headwater catchments have on the quality and quantity of their water resources. However, few studies have performed detailed observations on the effects of thinning on the groundwater flow process, especially over a long-term period of time. Also, to properly understand the water age in the scope of hydrological processes in forested areas, the combined use of different tracers is still not applied in many studies.

Estimating the water age of spring and groundwater in mountainous headwaters is important for evaluating the origins, the flow path and the storage volume of groundwater. Particularly in mountainous headwaters where relatively young spring and groundwater with ages of several years to several decades predominate, the inert gas sulfur hexafluoride (SF_6) is useful as a tracer for age-dating. SF_6 is a chemically stable human-made substance, and since its concentration in the atmosphere has increased since the 1950s, it is possible to estimate the apparent age of springs and groundwater for about 1 to 50 years.

The mean transit time (MTT) is also an important aspect of research related to water age. It is the time that elapsed between water entering a system and then leaving it, such as from the infiltration of precipitation into a catchment until its spring water discharge. In order to find the MTT, hydrogen and oxygen (^{18}O and ^{2}H) stable isotopes of water are most frequently used, and can estimate the MTT of water from the unsaturated zone to the outflow of rivers and springs.

In this study, we applied a new methodology that utilized a combination of stable isotopic concentrations of water and SF_6 atmospheric concentrations to investigate temporal variations in the spring water and groundwater mean transit time (MTT) of a forested headwater catchment in Japan.

The main objective of this study was to clarify how the characteristics of a forest alter its short and long-term hydrological processes in a headwater catchment. In order to do that,

understanding the change of MTT of spring water and groundwater is essential. We applied a new multi-tracer methodology that included analyses of stable isotopes of water and SF_6 atmospheric concentrations. Previous studies have mainly used trial-and-error approaches to identify the water age. We propose a new method that provides more reliable MTT estimation, as the model parameters are calibrated beforehand using apparent age information based on the SF_6 data. Using past and current hydrological and tracer data, we sought to effectively understand how short and long-term temporal changes in MTT after forest thinning in Japan.

The study area is at Mount Karasawa, from the Tokyo University of Agriculture and Technology Experimental Forest in Sano City, Tochigi Prefecture, Japan. On October 2011, a 50% linear thinning was applied on the plantation forest there. Stable isotopes of water and SF_6 analysis and hydrological observations were applied to investigate the temporal variation of MTT on three different time periods: “Before Thinning”, from June 2010 to September 2011, “Soon After Thinning”, from November 2011 to December 2013 and “Long After Thinning”, from August 2017 to November 2021. Field survey observations and sampling of spring water, groundwater (at 15m depth, GW15, and at 30m depth, GW30), groundwater level, discharge and runoff flow rate, etc. at biweekly or monthly intervals were conducted.

The SF_6 concentrations were used to estimate the apparent age of the spring water and groundwater, which were used to initiate a parameter calibration and model fitting process. This apparent age is an initial parameter that can be found from previous data analysis and, therefore, it is an educated estimate. The MTT was evaluated by estimating the d-excess variations of the stable isotopes of water using the exponential piston flow model (EPM), which is a Lumped-Parameter Model.

The MTT of spring water, GW15 and GW30 ranged from 40 to 55 months, 38 to 67 months and 34 to 62 months, respectively. In all of them, there is a tendency of MTT to increase soon after the forest was thinned. In contrast, the MTT was shorter approximately 4 to 8 years after thinning occurred. Considering that it is possible to assess the groundwater storage volume with

the MTT and spring water discharge knowledge, we found that the average volume of the catchment increased from 676 mm to 1,171 mm one to two years after the forest was thinned and approximately six years later, the storage volume was decreased to 588 mm. Therefore, the higher MTT values indicate an increase in groundwater volume storage and alteration of subsurface flow, and shorter MTT values indicate a decrease in groundwater volume storage and hydrological processes gradually returning to conditions similar to before the thinning of the forest.

The results indicate that the characteristics of the hydrological processes in the catchment underwent short and long-term changes after the forest was thinned. This study demonstrates that using combined tracer methods to investigate the hydrological response to forest treatment practices improved the results and can be used for better forest and subsurface water resources management.

Keywords: mean transit time; spring water; groundwater; stable isotopes; SF_6; tracers; forest thinning

Table of Contents

Abstract 4

Table of Contents 7

List of Tables and Figures 9

Tables 9

Figures 10

CHAPTER 1 INTRODUCTION 13

1.1 Water Background Studies 13

1.2 Forest Thinning and Hydrological Processes 15

1.3 Importance of Hydrological Research on Forest Areas 17

1.4 Hydrological Processes in Mountain Headwater Catchments 17

1.5 Water Age and Mean Transit Time Estimation 18

1.6 Tracers on Water Dating Studies 19

1.7 Objectives 23

CHAPTER 2 STUDY AREA 25

2.1 Overview of the Study Area 25

2.2 Study Period 26

CHAPTER 3 METHODS 33

3.1 Field Observation and Water and Air Sampling 33

3.2 Analysis of Dissolved Inorganic Components and Stable Isotopes of Hydrogen and Oxygen 37

3.3 Concentration of Sulfur Hexafluoride (SF_6) 38

3.3.1 Analysis of the Atmospheric Concentration of SF_6 38

3.3.2 SF6 Apparent Age Analysis 45

3.4 Selection of the Best Mean Transit Time (MTT) Model 48

3.5 Mean Transit Time (MTT) Estimation Model 48

3.6 Model Calibration and Fitting Process 50

CHAPTER 4 RESULTS 52
4.1 Hydrological Characteristics of the Headwater Catchment 52
4.1.1 Long-term Changes of Runoff and Groundwater Level 52
4.1.2 Stable Isotopes of Water Variation in Precipitation, Groundwater and Spring Water 57
4.2 SF_6 Apparent Age and the Weighted Average 66
4.3 Isotopic Content in Precipitation 72
4.4 Spring Water and Groundwater Mean Transit Time 72
4.5 Long-term Hydrological Processes at the Study Area 89
CHAPTER 5 DISCUSSION 92
CHAPTER 6 CONCEPTUAL MODEL 98
CHAPTER 7 CONCLUSIONS 101
ACKNOWLEDGMENTS 103
References 104
ANNEX 112

List of Tables and Figures

Tables

Table 1. Descriptions of the KS2-5 catchment 31
Table 2. Coefficient (SF_6) used to calculate the constant of proportionality (IAEA, 2006) 433
Table 3. Annual water balance at the Mount Karasawa study area. 555
Table 4. Annual Precipitation (P, in mm), Stream Runoff (R, in mm) and Runoff Ratio at the Mount Karasawa study area. 566
Table 5. Observed d-excess (‰) distribution in precipitation Before Thinning, Soon After Thinning and Long After Thinning. 61
Table 6. Observed d-excess (‰) distribution in spring water Before Thinning, Soon After Thinning and Long After Thinning. 62
Table 7. Observed d-excess (‰) distribution in groundwater at 15m deep Before Thinning, Soon After Thinning and Long After Thinning. 633
Table 8. Observed d-excess (‰) distribution in groundwater at 30m deep Before Thinning, Soon After Thinning and Long After Thinning. 644
Table 9. Observed d-excess (‰) distribution in stream water Before Thinning, Soon After Thinning and Long After Thinning. 655
Table 10. Sampling dates, apparent SF_6 age of each sample (in months) and their daily discharges (in mm/day). The weighted average of the apparent ages is 39.1 months. 70
Table 11. Sampling dates, apparent SF6 age of each sample (in months) and their daily discharges (in mm/day). The weighted average of the apparent ages is 33.51 months. 71
Table 12. Final parameters of the EPM after the fitting process, for each water sampled and study period. The MTT is represented by the τ parameter in months. The precipitation input function is $din\ (t) = 12.35 + 13.42 \sin(0.52t)$. 888

Figures

Figure 1. Long-term changes in northern hemisphere mean atmospheric sulfur hexafluoride (SF6) concentrations, chlorofluorocarbons (CFCs), and tritium (^{3}H) concentrations in precipitation over Washington, D.C. (1950 ~ 2017). Created based on the USGS (United States Geological Survey). (From Suzuki, 2022) 222
Figure 2. Map of the study area showing the KS2-5 catchment (red boundary) where the spring water and groundwater data were collected, as well as the nearby KS2-4 catchment (green boundary) where stream water and precipitation data were collected. 277
Figure 3. Spring point of KS2-5 catchment (KS2-5 SP) (May 26, 2021) 288
Figure 4. Observation wells in the KS2-5 catchment (Left: GW15, Right: GW30) (November 26, 2020) 299
Figure 5. Cross section of the catchment area from the observation wells to the spring point and geological characteristics 30
Figure 6. Landscape of catchment after a 50% linear thinning 322
Figure 7. Spring water flow rate observation (January 27, 2021) 366
Figure 8. Overview of Dissolved Sulfur Hexafluoride Analysis System (From Sakakibara, 2018) 422
Figure 9. Annual changes in atmospheric concentration of sulfur hexafluoride (SF6) in the study area. The black straight line is the northern hemisphere mean (NOAA and USGS), and the red straight line is the proportional correction of the northern hemisphere mean. (From Suzuki, 2022) 444
Figure 10. Air conversion lines (Mt. Karasawa area and North Hemisphere), according to the SF_6 concentrations in the air obtained in the study area, which indicate the recharge year of each water sample 477
Figure 11. Stream water precipitation and runoff measurements, groundwater (GW) levels measured in the two boreholes, during the observation period (June 2010–November 2021). The forest was 50% thinned in October 2011. 544
Figure 12. Long-term variations in spring water and groundwater stable isotopes of oxygen-18 (δ18O‰) during the observation period (June 2010–November 2021). 588
Figure 13. Long-term variations in spring water and groundwater stable isotopes of deuterium (δ^2H‰) during the observation period (June 2010–November 2021). 599

Figure 14. Long-term variations in precipitation, spring water and groundwater d-excess of stable isotopes during the observation period (June 2010–November 2021).....60
Figure 15. Concentration of sulfur hexafluoride (SF_6) in spring water and groundwater Concentrations before atmospheric conversion are shown (From Suzuki, 2022).....699
Figure 16. Precipitation d-excess and fitted line Before Thinning. 755
Figure 17. Precipitation d-excess and fitted line Soon After Thinning.....766
Figure 18. Precipitation d-excess and fitted line Long After Thinning. 777
Figure 19. Variations in the spring water d-excess and MTT analysis flow applying the EPM to fit the observed data Before Thinning. 788
Figure 20. Long-term variations in the spring water d-excess and MTT analysis flow applying the EPM to fit the observed data Soon After Thinning.....79
Figure 21. Long-term variations in the spring water d-excess and MTT analysis flow applying the EPM to fit the observed data Long After Thinning. 80
Figure 22. Variations in the groundwater 15 m d-excess and MTT analysis flow applying the EPM to fit the observed data Before Thinning.....8181
Figure 23. Variations in the groundwater 15 m d-excess and MTT analysis flow applying the EPM to fit the observed data Soon After Thinning.....822
Figure 24. Variations in the groundwater 15 m d-excess and MTT analysis flow applying the EPM to fit the observed data Long After Thinning.....833
Figure 25. Variations in the groundwater 30 m d-excess and MTT analysis flow applying the EPM to fit the observed data Before Thinning.....844
Figure 26. Variations in the groundwater 30 m d-excess and MTT analysis flow applying the EPM to fit the observed data Soon After Thinning.....855
Figure 27. Variations in the groundwater 30 m d-excess and MTT analysis flow applying the EPM to fit the observed data Long After Thinning.....866
Figure 28. Variations in the stream water d-excess and MTT analysis flow applying the EPM to fit the observed data Long After Thinning. 877
Figure 29. Schematic diagram illustrating hydrological processes in the study area during the "before thinning" (2010–2011), "soon after thinning" (2011–2013), and "long after thinning" (2017–2021) study periods. Arrow lengths demonstrate changes in the amount of water loss and infiltration, with the precipitation arrow remaining stable. The water table line indicates fluctuations in groundwater storage. The MTT and volume are shown below the diagram.....91
Figure 30. Comparison of high rainfall events from Chiu et al., 2022 and this study. 977

Figure 31. Schematic diagram illustrating the hydrological processes in the study area during the observation period. The number of arrows demonstrate the changes in the amount of ET, Q and I, with the P arrow remaining stable. The water table line indicates fluctuations in groundwater storage volume. 100100

CHAPTER 1 INTRODUCTION

1.1 Water Background Studies

Water is essential to life. It is of utmost importance to avoid its scarcity and guarantee a sustainable future to all people around the world. Increasing water efficiency and improving water management are critical to balancing the competing and growing water demands. Hence, one of the United Nation focus of their Sustainable Development Goals is the number 6, which is to ensure availability and sustainable management of water and sanitation for all (United Nations, 2019). Scarcity of groundwater and surface water is currently a problem faced by communities all over the world (Newton *et al*., 2015). Problems concerning water resources quantity and quality need to be solved by deciding the best ways to use and conserve this precious natural resource.

Globally, there is an increasing demand for groundwater resources to support Earth's population, and in turn, there is an increasing reliance on groundwater and the need to understand regional scale flow system (Gleeson *et al*., 2012).

The main factors that control groundwater and surface water supply are climate and geology, with precipitation providing the primary water input, and the geology controlling how water moves from the recharge area and headwaters to where it is used. Currently, it is not possible to alter either climate or regional geology in a controlled manner, but there are ways to increase the amount of available water, by altering vegetation patterns and or the landscape. Changes in forest structure due to management can affect the forest water balance (Komatsu *et al*., 2007). With this kind of alterations, it is possible to change the amount of water that infiltrates into the groundwater and surface water systems.

Approximately 65% of Japan is forested, with 40% of these forested lands being plantation forests, and Japanese cedar and Japanese cypress being the most commonly planted tree

(Forestry Agency, 2017). Without forest management practices such as thinning, the extensive canopy coverage of these trees prevents sunlight from reaching forest floors thus preventing growth of understory vegetation (Kuraji *et al*., 2019).

Natural and human induced land use changes are expected to change hydrological behavior significantly and are thus a major concern for water quality and quantity (Klaus and McDonnell, 2013).

Direct quantification of catchment storage remains difficult because of its largely unobservable nature and the subsurface spatial heterogeneity within and among catchments (Lazo, *et al*. 2019). Few studies too have yet quantified the relation between catchment storage and catchment features (e.g., rainfall temporal variability, vegetation, soils, geology) and this remains an open question in hydrology science (McNamara *et al*., 2011).

Still, more information is needed about the subsurface contact time in small watersheds to make predictions about stream water chemical changes from land-use and environmental change (McGuire *et al*., 2002). And observing the temporal changes after forest thinning will be required of future researches to evaluate the effects of forest management on water resources over time (Sun *et a*l., 2015).

Finally, some authors suggest that, the combined information from stable isotopes of water with CFCs and SF_6 (which is a multi-tracer approach) can provide valuable insight into the mechanism and movement of water (Kamtchueng *et al*., 2017). Also, future studies should investigate thinning and subsurface runoff on the hydrological impacts over the longer-term (post-thinning recovery phase) (Kuraji *et al*., 2019).

1.2 Forest Thinning and Hydrological Processes

As it was mentioned previously, a large area of Japan's land is covered by forest plantations made of cedar and cypress. Japanese cypress (*Chamaecyparis obtusa*) and Japanese cedar (*Cryptomeria japonica*), the two major coniferous species, were planted mainly after the Second World War to meet the high demand for timber in Japan (Iwamoto, 2002).

However, in the past decades, there has been a combination of decreasing forest workers and increasing of cheap wood resources from foreign countries, which has led to a poor forest management in Japan. Hence, the forests have sparse or no understory vegetation cover due to the low light conditions that commonly occur under the dense forest canopy, particularly in Japanese cypress forests (Onda *et al*., 2010).

The Japanese archipelago is covered by forests that are mainly located in mountainous areas, wherein forested headwaters play a substantial role in supplying water to lowland areas (Momiyama *et al*., 2021).

Almost half of these forested areas are plantation forests, mainly of Japanese cedar and Japanese cypress, and have a lack of management, which can result in a wide canopy coverage that increases soil erosion, for instance (Kuraji *et al*., 2019). According to (Pereira *et al*., 2022), forest restoration and soil restoration dynamics, as well as hydrological process conservation, are sparsely studied. Also, (Lu *et al*., 2022) stated that water scarcity or abundance is an important factor in forest degradation, and no detailed analysis of forest degradation and soil characteristics has been conducted.

These plantation forests lack management, which affects hydrological processes in the forests. To address these management deficiencies and improve water conservation, forest thinning could be applied (Nam *et al*., 2016). Forest thinning can alter the water balance and flow paths, thereby affecting water availability, quality, and supply (Kuraji *et al*., 2019).

Thinning of forests, which is the cutting of trees to improve the functions of a forest, made

not only with the purpose of wood production, is expected to improve water resources problems. Thus, forest thinning alters the stand structures (e.g., more open forest canopies and the recovery of understory vegetation) and modifies the climatic and soil conditions within the stand (e.g., higher light penetration and soil water content) (Molina and del Campo, 2012). Also, it can modify the water balance and flow path, which in turn affect water availability, quality and supply rate to downstream users (Kuraji *et al*., 2019).

The effect of thinning on groundwater level has been discussed in recent researches, as showed in Komatsu *et al*., 2010 and Hotta *et al*., 2010, especially in Japan, where forest management treatments, such as thinning, has been performed to increase water resources. Some results have reported the effect of thinning on storm runoff, for example, Dung *et al*., 2012, has stated that forest thinning changes the cover and structure of the forest canopy and plays an important role in regulating the hydrological cycle at multiple temporal and spatial scales.

Thinning also usually increases the supply of rainwater to the forest floor by reducing canopy interception loss (Lane and Mackay, 2001). Considering that, in some areas tree thinning causes canopy interception to decrease, making more rainwater reach the ground and potentially infiltrate through the soils and. Therefore, thinning of a forest can be used not only for wood production but to improve water resources quantity and quality.

Other studies also emphasize the importance of research on forest thinning. Kuraji *et al*., 2003 reported that abandoned plantations could consume more water from their dense canopies because of a higher evapotranspiration rate and thus reduce catchment runoff and water resources.

Sun *et al*., 2015, observed a higher throughfall amount in annual canopy water balance from pre-thinning (61.4%) to the post-thinning (73.0%) period; overall, thinning caused throughfall rate to increase and stemflow rate and canopy interception rate to decrease. These authors also have stated that an understanding of the relationship between the canopy water balance and the forest would play an important role in accurately predicting how forest management affects

rainfall partitioning and, consequently, water resources.

1.3 Importance of Hydrological Research on Forest Areas

Numerous studies have been conducted on the thinning effect on evapotranspiration in plantations in Japan. However, such findings have not been reflected using rainfall-runoff models. How thinning may affect runoff under a large variety of precipitation and soil hydrological conditions.

There are many studies showing the forest cover change and runoff response relationship. But it is difficult to predict water yield because of the variety of areas' characteristics. And there are few studies on the impact of groundwater recharge and yield.

The potential impact of forest thinning on groundwater recharge and water age and related springs has largely been ignored until recently.

Considering that the relationship between thinning and subsurface processes is not clear yet, especially regarding the MTT, this research is very significant for hydrological studies on forest areas.

1.4 Hydrological Processes in Mountain Headwater Catchments

It is important to understand the time from the recharge of groundwater to the discharge as surface water in the mountain headwater catchments, which is the main recharge area of groundwater resources. By estimating the route and water age, it becomes possible to use groundwater resources sustainably and manage them appropriately.

In mountainous headwaters, it is said that the origin of runoff and groundwater flow system change, especially during rainfall events. Muñoz-Villers and McDonnell (2012) identified the origin of groundwater and estimated its flow path due to an increase in discharge during a rainfall

event. During the process of recharging groundwater, it infiltrates through the ground and becomes a eugenic recharge source of groundwater, increased from 15% to 55%. Cartwright and Morgenstern (2018), on the other hand, found that soil water preferentially contributes to runoff as it increases during rainfall events in watersheds predicted to have macropores in unsaturated zones and low-permeability soil layers. In order to determine the amount and timing of rainfall runoff, it is important to understand the runoff characteristics of groundwater during rainfall events, that is, the origin of runoff water and the groundwater flow system in the rainfall runoff process.

Marui (1991) reported on the slope near the valley in the forest sub-catchment of the headwaters of the Tama Hills. It was confirmed that a groundwater ridge was formed in the lower part of the Kanto loam layer when water was brought in by continuous rainfall. It was clarified that groundwater bodies extend above the Kanto Loam Formation and surface currents are generated, and the hydrological processes inside the volcanic edifice, which are the main causes of surface currents during the rainfall runoff process, were clarified. In this way, it is predicted that the groundwater flow system will undergo complex changes due to various field conditions and the occurrence of rainfall events in mountain headwater basins.

1.5 Water Age and Mean Transit Time Estimation

To understand how forest thinning affects hydrological processes, it is important to know the mean transit time (MTT) of spring water and groundwater over a long period. Transit time is the amount of time elapsed from when water enters a system until it leaves the system, e.g., from when precipitation infiltrates into a catchment until it is discharged as spring water (McGuire and McDonnell, 2006). In this study, we argue that using an estimated MTT provides useful information regarding the effects of forest thinning, as MTT provides vital details on hydrological processes, including storage at a catchment scale and initial approximations of catchment transport behavior (Sprenger *et al*., 2019).

The MTT can be modeled by the relationship between precipitation and hydrological components using conservative tracers (Asano *et al*., 2002; Kabeya *et al*., 2007; Jung *et al*., 2020). In this study, we used ^{2}H and ^{18}O (stable isotopes of water) as conservative tracers to estimate the MTT (Herrmann *et al*., 1990).

Previous studies have shown that estimating the MTT using multi-tracer analysis provides complementary insights into hydrological processes (Soulsby *et al*., 2009; Jung *et al*., 2020; Zhou *et al*., 2021). In particular, sulfur hexafluoride (SF_6) concentrations in the air and $^{2}H/^{18}O$ are commonly used tracers and have been applied effectively in multi-tracer studies (Stadler *et al*., 2010; Kamtchueng *et al*., 2017). However, the combined application of SF_6 and $^{2}H/^{18}O$ in forests undergoing thinning has not been addressed previously.

The chemical stability of SF_6 and its continuously increasing concentrations in the Northern Hemisphere make it an effective tracer for groundwater recharge (Busenberg and Plummer, 2000; Stewart *et al*., 2018; Sakakibara *et al*., 2019). Therefore, a multi-tracer approach could improve the robustness of age interpretations and the current understanding of groundwater recharge processes.

1.6 Tracers on Water Dating Studies

In estimating the water MTT, there is a method using environmental tracers. Hydrogen and oxygen stable isotopes are most frequently used, and can estimate the time of groundwater from the unsaturated zone to the outflow of rivers and springs. The stable isotope ratio (d-excess value) in precipitation, which shows seasonal variations throughout the year, is due to the mixing of groundwater with various isotope ratios in the process of precipitation recharging groundwater and flowing. It is possible to estimate the residence time using a groundwater mixing model by using the isotope ratio of precipitation and the attenuation of the isotope ratio of runoff.

Kabeya *et al*. (2007) found that soil water and groundwater ages were estimated over a range of 0 to 9 months. It was shown that isotopes are useful in their study. Stewart *et al*. (2010), using this stable isotope ratio decay width, pointed out that the time required by a groundwater mixing model is up to four years.

In catchments where mixing is expected, it is also important to determine the water age and MTT by using other tracers. Therefore, a method of estimating the residence time using inert gases such as SF_6 (sulfur hexafluoride) and stable isotopes as tracers can been applied.

The use of SF_6 is said to be useful as one of the methods for estimating the groundwater age (Sakakibara *et al*., 2017; Asai *et al*., 2011). SF_6 is a chemically stable environmental tracer and has been increasing in the atmosphere since the 1980s (Figure 1).

Busenberg and Plummer (2014) conducted long-term observations of spring water ages in the Blue Ridge Mountains, one of the mountainous headwater basins in the United States, for 17 years. It was clarified that the age estimated by SF_6 is older than that in the summer season with high precipitation due to the increase in the ratio of spring outflow of recharged and stored groundwater in the summer season.

In addition, Sakakibara (2018) confirmed that the hydraulic gradient from the observation well to the spring point increased by about 10% during the rainfall event in the mountain headwater basin of the granite basin compared to before the rainfall event. Under such conditions, the retention time estimated by SF_6 was more than 10 years compared to before the rainfall event, indicating the possibility that deep groundwater contributed to the outflow of spring water. In this case, it is necessary to predict the ground environment such as recharge temperature and recharge altitude at the time of groundwater recharge.

Hydrological processes have been analyzed by researchers based on spatial and component-based information, but, unfortunately, there are few studies incorporating the time scale (age information) in the groundwater component (Sakakibara *et al*., 2019).

MTT can be estimated by analyzing the isotopes of water molecules. For the water in

precipitation becomes isotopically distinct as it flows through the system, until it goes into the subsurface, and then exits with a different isotope signature.

Investigations have been aimed at using stable isotopes to determine the distributed groundwater recharge rate (Vachier *et al*, 1987), and recharge mechanisms (Darling and Bath, 1988). According to Kendall and McDonnell, 2012, stable isotopes provide a powerful tool for understanding the movement of water through catchments and ecosystems.

In order to do such investigations, the main study is targeted to the stable isotopes of water. The environmental isotope ^{2}H (or D, for deuterium) and ^{18}O (oxygen-18) are constituents of the water molecule and, therefore, ideal (conservative) tracers in the water cycle (Herrmann *et al*., 1990).

Hydrological studies that focus on isotopes are based on the notion of tracing a water molecule through the hydrological cycle and so, stable isotopes of water (^{2}H and ^{18}O) have been used since the innovative work of Craig, 1961. According to Kendall and Caldwell, 1998, these tracers are applied by precipitation and are generally distinct isotopically, which makes them reliable tracers of subsurface flow processes.

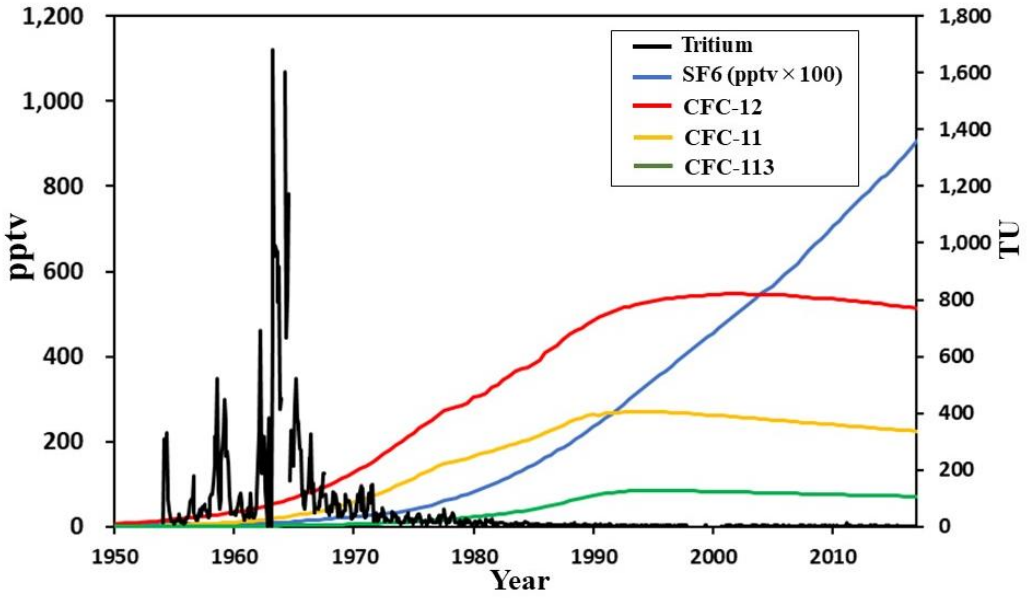

Figure 1. Long-term changes in northern hemisphere mean atmospheric sulfur hexafluoride (SF6) concentrations, chlorofluorocarbons (CFCs), and tritium (3H) concentrations in precipitation over Washington, D.C. (1950 ~ 2017). Created based on the USGS (United States Geological Survey). (From Suzuki, 2022)

1.7 Objectives

The main objective of this study was to clarify how the characteristics of a forest alter its short and long-term hydrological processes in a headwater catchment. In this study, we argue that estimated MTT provides useful information regarding the effects of forest thinning, as MTT offers vital details on hydrological processes, including storage at a catchment scale (McGuire and McDonnell, 2006) and initial approximations of catchment transport behavior (Dung *et al*, 2015). We applied a new multi-tracer methodology that included analyses of stable isotopes of water and SF_6 concentrations of the air. Previous studies have mainly used trial-and-error approaches to identify the water age (McGuire and McDonnell, 2006; Asano *et al*, 2002; Kabeya *et al*, 2007; Jung *et al*, 2020). This study aims to provide more reliable MTT estimates, as the model parameters are calibrated beforehand using apparent age information based on the SF_6 data.

We applied a new multi-tracer methodology that included analyses of stable isotopes of water (^{18}O, ^{2}H) and SF_6 atmospheric concentrations. Previous studies have mainly used trial-and-error approaches to identify the water age. We propose a new method that provides more reliable MTT estimates, as the model parameters are calibrated beforehand using apparent age information based on the SF_6 data. Using past and current hydrological and tracer data, we sought to effectively understand how short and long-term temporal changes in MTT after forest thinning in Japan.

The main points that we aim to understand with this research are:

- Investigation of short and long-term variations in the spring water and groundwater MTT after forest thinning;
- The use of a multi-tracer analysis that improves the MTT estimation process;
- Clarify the effects of forest thinning on short and long-term hydrological processes, after forest thinning in Japan.

This type of research is important to quantitatively evaluate the effect of forestry practices and treatments in forested catchments. By understanding such processes, it could be possible to predict in what way forest management affects spring water and groundwater MTT mean residence time and, consequently, water resources. Thus, this work can benefit a better understanding of headwater forested catchments management.

CHAPTER 2 STUDY AREA

2.1 Overview of the Study Area

The study area is the small headwater catchment (KS2-5 catchment) in the Tokyo University of Agriculture and Technology Karasawa Forest in Tanuma-cho, Sano City, Tochigi Prefecture (Figure 2). The KS2-5 catchment has an elevation above sea level of 181 m to 271 m and an area of 0.01 km^2. There is a spring point (Figure 3) and there are two observation groundwater wells with a depth of 15m (GW15) and 30m (GW30) that can be seen on Figure 4.

The basement geology is sandstone and chert of the Chichibu Paleozoic Formation, but it is believed that cracks due to weathering are dominant. (Kawaguchi, 2013). The geological structure and hydraulic conductivity (m/s) of two observation wells installed have been confirmed by a field drilling core survey in 2010.

Kawaguchi (2013) conducted a survey test and a simple penetration test up to an observation well and a spring (195 m a.s.l. point). Although it is sandstone in the sedimentary bed, cracks are prominent due to weathering, and it is believed that the groundwater inside the basement rock flows through the cracks as a water channel. (Figure 5).

Meteorological observations are being made by the Japan Meteorological Agency at a point about 5.5 km southwest of the target area. The average annual temperature is 14.5 °C and average annual rainfall is 1245 mm (Table 1).

The vegetation in the target basin is mainly artificial forests of Japanese cedar and Japanese cypress planted around 1966. In order to quantitatively evaluate the effect of forest management treatments in forested watersheds before and after thinning conditions, a 50% intensity thinning was performed at the study area in the KS2-5 catchment on October 2011. The type of treatment was a line thinning, in which two lines of trees were cut and two lines were left uncut (Figure 6)

2.2 Study Period

Forest thinning management throughout the Mount Karasawa area included tree cutting in July 2011 and landing and transporting in October 2011 (Dung *et al*., 2015). In the study area, 50% intensity linear thinning was performed in the KS2-5 catchment forests in October 2011. The study period was divided into three parts: “Before Thinning” (June 2010–September 2011), “Soon After Thinning” (November 2011–December 2013), and “Long After Thinning” (August 2017–November 2021).

As mentioned before, the aim of this study was to understand the short and the long-term temporal variations in MTT. Therefore, we analyzed the study period according to the thinning treatment. That way, we can interpret what happens to the hydrological processes of a forest and compare those changes before the thinning of trees, soon after that and a long time after that treatment.

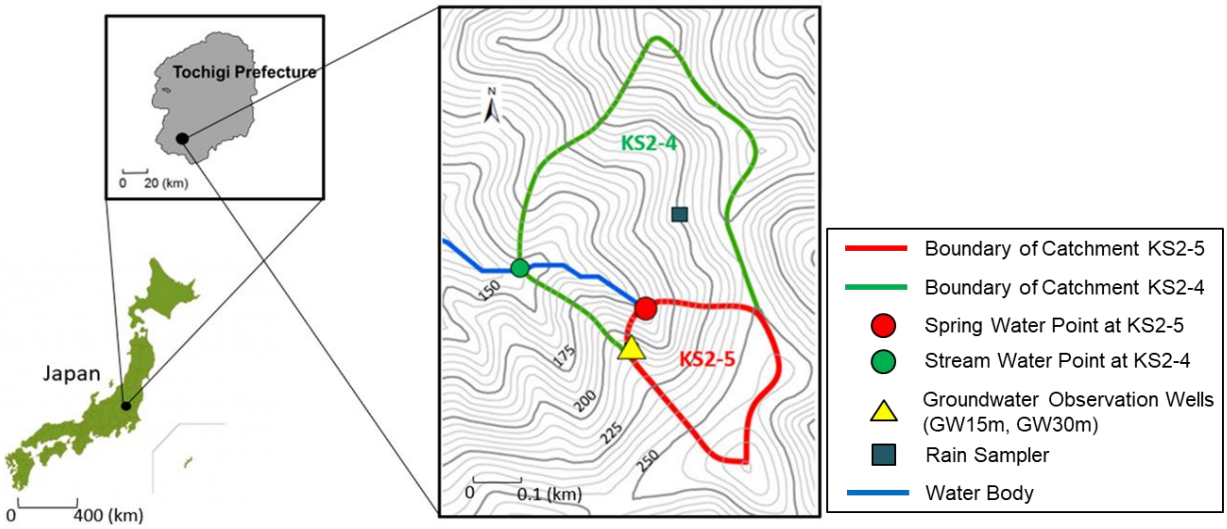

Figure 2. Map of the study area showing the KS2-5 catchment (red boundary) where the spring water and groundwater data were collected, as well as the nearby KS2-4 catchment (green boundary) where stream water and precipitation data were collected.

Figure 3. Spring point of KS2-5 catchment (KS2-5 SP) (May 26, 2021)

Figure 4. Observation wells in the KS2-5 catchment (Left: GW15, Right: GW30) (November 26, 2020)

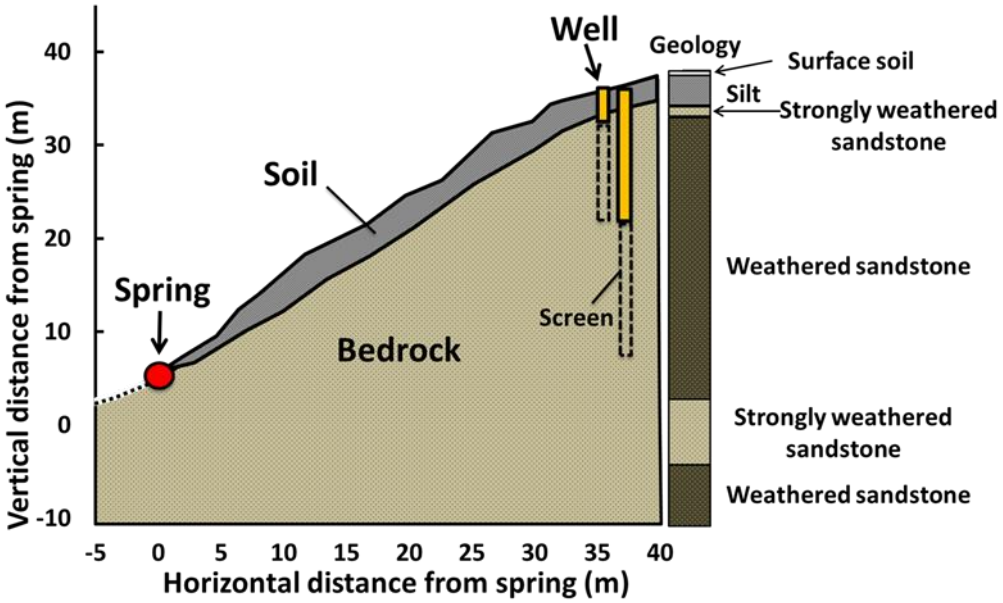

Figure 5. Cross section of the catchment area from the observation wells to the spring point and geological characteristics

Table 1. Descriptions of the KS2-5 catchment

	KS2-5 catchment
Area	0.01 km^2
Elevation range	181 - 271 m
Slope angle	55%
Vegetation cover	Japanese Cedar/Sugi, Cypress/Hinoki
Soil thickness	35 - 200 cm
Geology	Sandstone
Average annual temperature	14.5 °C
Average annual precipitation	1245 mm

Figure 6. Landscape of catchment after a 50% linear thinning

CHAPTER 3 METHODS

3.1 Field Observation and Water and Air Sampling

Continuous hydrological observations and measurements have been done in the KS2-5 catchment since 2010. This current research's field survey was conducted at a monthly frequency during the period from August 2017 to August 2019 and at a biweekly frequency from August 2020 to November 2021.

Spring water, rainwater, stream water and groundwater (from GW15 and GW30) were sampled for stable isotope and SF6 analyses mainly, and other additional hydrological measurements.

The water samples were collected in 100 mL plastic containers (stable isotope analyses) and 500 mL amber glass bottles (SF_6 analyses). To collect the water sample for SF_6 analysis, the bottle and cap were placed in a 2 L volume bucket with water overflowing from it. When sampling, it was necessary to prevent contamination with the atmosphere, so we pumped up the water at the spring point and groundwater well and confirmed that there was no air intrusion in the samples.

On the field surveys, water temperature, electrical conductivity (EC), pH, oxidation reduction potential (ORP), Dissolved oxygen (DO) was measured using a water thermometer (TX1001, Yokogawa Meters & Instruments Corporation), a conductivity meter (D-54, electrode 9382-10D, Horiba Ltd.), pH meter (D-54, electrode 9625-10D, Horiba), redox potential meter (D-55, electrode 9 300-10D, Horiba), dissolved oxygen concentration meter (D-55, electrode 9551-20D, Horiba, Ltd.) was used.

The pH meter was calibrated in advance for pH = 4 and 7. The dissolved oxygen concentration measuring instrument was calibrated by measuring the atmosphere. A handheld GPS (eTrex 30, GARMIN) was used.

The flow rate of spring water was measured directly below the water sampling point. Water

was sampled with a 45 L plastic bag for a certain period of time, and the flow rate was measured with a graduated cylinder (Figure 7). By repeating the measurement three times or more, the average flow rate was calculated.

The groundwater level at the observation well was observed at intervals of 10 minutes to 1 hour using a water level and temperature logger (HOBO CO-U20-001-01; Tempcom instrumentation Ltd., UK) was used for the observations and another one of the same type was used to correct the atmospheric pressure from the measured water, which was installed near the observation wells. In order to compensate for this, an atmospheric pressure gauge was installed near the observation well and the atmospheric pressure was also measured. Based on the water level, it was converted to the groundwater level.

Two types of buckets, one made of plastic and the other made of stainless steel, were used when sampling groundwater. One 100 mL plastic container was used for analysis of dissolved inorganic components and hydrogen/oxygen stable isotope ratio analysis, and three 500 mL brown glass bottles were used for sulfur hexafluoride (SF_6) concentration analysis.

To collect the water sample for SF_6 analysis, a cap and a 500 mL amber glass bottle were placed in a corkscrew with a volume of 2 L, spring water was pumped up with a tube pump, and introduced into the corkscrew using a nylon tube connected to the tube pump. When sampling water for analysis, it was necessary to prevent contamination with the atmosphere, so we pumped up the water at the spring point as much as possible and confirmed that air was not flowing with the water from the nylon tube outlet. After introducing corkscrew, overflow the spring water and replace the water in the glass bottle sufficiently. After that, the cap was wrapped with butyl rubber tape about three times from the end of the cap and stored.

A 100 mL glass syringe (glass syringe, VAN) and a three-way stopcock (Telfation three-way stopcock L-lock connector (TS-TL2K), TERUMO) were used to collect air samples in the catchment area. After sealing with a three-way stopcock, the tube was kept pressurized with vinyl tape and brought back to the laboratory.

Both the stable isotopes and SF_6 dissolved concentration analyses were done in the Hydrology and Water Environment Laboratory, Faculty of Life and Environmental Sciences, University of Tsukuba, Japan.

Figure 7. Spring water flow rate observation (January 27, 2021)

3.2 Analysis of Dissolved Inorganic Components and Stable Isotopes of Hydrogen and Oxygen

Inorganic dissolved component analysis targeted a total of 9 components, including Na^+, K^+, Ca^{2+}, and Mg^{2+} as cations, and Cl-, HCO_3^-, NO_3^-, SO_4^{2-}, and SiO_2 as anions. After filtering the water sample with a 0.20 μm cellulose ester filter (DISMIC－25, ADVANTEC), anions except HCO_3^- were subjected to ion chromatography (HIC－10Asuper, Shimadzu), and cations and Si were analyzed by the Center for Research Infrastructure, University of Tsukuba.

The plasma emission spectrometer (ICP-8100, PerkinElmer) of the department was used for analysis. For Si, the concentration was converted to SiO2 concentration after analysis. For HCO3 concentration analysis, pH 4.8 alkalinity titration using 0.005 mol sulfuric acid solution was applied.

Because air masses over Japan cause seasonal variations in rainfall, we used the d-excess of ^2H and ^{18}O (stable isotopes of water) as conservative tracers to estimate the MTT (Chiu *et al.*, 2022). Stable isotope ratios were analyzed using a liquid water isotope analyzer (L2120-i, Picarro) using wavelength scanning cavity ring-down spectroscopy. The results are expressed as δ values (‰) as shown in Equation 1 (Coplen, 1994):

$$\delta\,(‰) = \frac{R_{Sample} - R_{SMOW}}{R_{SMOW}} \times 1000 \quad (1)$$

R_{SMOW} indicates $^{18}O/^{16}O$ or $^2H/^1H$ in V-SMOW (Vienna-Standard Mean Ocean Water), and RSample indicates $^{18}O/^{16}O$ in the sample. The analytical accuracy is ±0.3‰ for $\delta^{18}O$ and ±1.0‰ for δ^2H.

3.3 Concentration of Sulfur Hexafluoride (SF_6)

3.3.1 Analysis of the Atmospheric Concentration of SF_6

The dissolved concentration of SF_6 was analyzed using the analysis system of the Water Circulation and Water Environment Laboratory, Faculty of Life and Environmental Sciences, University of Tsukuba. The analysis system consists of a separation/concentration device that separates SF6 from a water sample and then concentrates it, a detection device that detects the separated and concentrated SF6, and a data processing device. A carrier gas (high-purity N2 gas, purity of 99.99995% or higher) is used to bubble the introduced water sample. In this operation, SF6 is separated by high-purity N2 bubbles, moves to a trap column packed with packing material, and is concentrated. A tograph (GC-8A, Shimadzu) was used, and high-purity N_2 was used as the carrier gas in the same way as the separation and concentration equipment. A schematic diagram is shown in Figure 8.

The limit of quantification in SF_6 analysis is 0.1 fmol (Sakakibara *et al*., 2017). The same analytical system was used for the analysis of dissolved concentrations of SF_6 in air. After that, the dissolved SF_6 concentrations in water samples were analyzed by the same procedure. Water samples were analyzed by measuring the groundwater level and spring water 2 to 4 times, and air samples 4 to 5 times.

Henry's law was used to convert the dissolved SF_6 concentration in the water sample to the atmospheric concentration at the time of recharge. This law states that if there is no reaction between gases, the solubility in water is proportional only to the partial pressure of each gas.

$$C_i = K_{H_i}\, p_i \qquad (2)$$

Ci is the dissolved concentration, KHi is the constant of proportionality, and pi is the partial pressure. The IAEA (2006) provides a conversion method using Henry's law, and the method is shown below. According to this method, the dissolved concentration was converted to the

atmospheric concentration at the time of recharge. , can be estimated from Eq. (3) in areas below 3,000 m above sea level.

$$\ln P = - H/8300 \quad (3)$$

P indicates the total atmospheric pressure, and H indicates the recharge altitude. By defining it, we estimate the recharge elevation (Yasuhara *et al*., 2007; Asai *et al*., 2001). Since this study did not cover the entire volcanic edifice, the recharge elevation in this study was set at 181 m a.s.l, the lowest elevation of the KS2-5 basin, and 271 m a.s.l, the highest elevation, referring to Kawaguchi (2013) was averaged to 226.0 m a.s.l. Since groundwater recharge occurs in the moist unsaturated zone, the relative humidity is close to 100%. Therefore, it is necessary to subtract the water vapor pressure from the total atmospheric pressure using Eq. (4) to calculate the mixing ratio of SF_6 in dry air.

$$p_i = x_i\left(P - p_{H_2O}\right) \quad (4)$$

xi is the molecular weight in dry air, and p_{H2O} is the water vapor pressure. This water vapor pressure p_{H2O} was calculated using equation (5).

$$ln\, p_{H_2O} = 24.4543 - 67.4509\left(\frac{100}{T}\right) - 4.8489ln\left(\frac{T}{100}\right) - 0.000544S \quad (5)$$

T is the recharge temperature and S is the salinity concentration. (Asai *et al*., 2010; Asano *et al*., 2011). In this study, we used the average monthly mean temperature for 19 years from 2000 to 2020 in Sano City, Tochigi Prefecture, which is published by the Japan Meteorological Agency. The reason for this is that the temperature of the spring water sampled in this study and Kashiwa (2019) was almost constant and tended to indicate the average temperature in Sano City, so the temperature at the time of recharge was set in this way. In addition, the KS2-5 basin

is located inland and is unlikely to be affected by the intrusion of seawater with high salinity or wind-blown salt. Therefore, the salinity was set to zero. The constant of proportionality K_H in Henry's law is determined by Eq. (6) using salinity and recharge temperature at standard atmospheric pressure of 1013.25 hPa.

$$\ln K_H = a_1 + a_2\left(\frac{100}{T}\right) + a_3 ln\left(\frac{T}{100}\right) + S\left[b_1 + b_2\left(\frac{T}{100}\right) + b_3\left(\frac{T}{100}\right)^2\right] \quad (6)$$

T is the recharge temperature, S is the salinity concentration, a1 to a3 and b1 to b3 are coefficients necessary for the calculation, and are applicable in the range of recharge temperature from 0 to 40℃ and salinity from 0 to 40%. Table 2 shows the coefficients used to calculate the constant of proportionality in the SF_6 analysis.

Excess air (EA) is defined as the dissolved air in excess of the solubility equilibrium with the atmospheric concentration during groundwater recharge. This is due to excessive dissolution of the atmosphere in the unsaturated zone (Gooddy *et al*., 2006).

During heavy rains such as typhoons, the groundwater level rises rapidly, and the air in the soil mixes with the groundwater, resulting in excess air volume. It is thought that it will increase (Sakakibara *et al*., 2017). Since excess air underestimates the residence time, it is an important factor in estimating the residence time.

In particular, SF_6 has a remarkably large correction factor for the amount of excess air, so its evaluation is an important issue (Sakakibara *et al*., 2017). Noble gases such as nitrogen, neon, and argon are used to estimate excess air, but there are almost no examples of measuring them in Japan. It has been confirmed that the soil in the KS2-5 catchment is formed with a thickness of about 30 cm to 200 cm above the bedrock (Kawaguchi, 2013).

Therefore, in this study, the value of EA was set to 0. Based on the above, the atmospheric concentration during recharge was calculated using equation (7), which takes into account excess air in Henry's law.

$$x_i = \frac{C_i}{K_H\left(P - p_{H_2O}\right) + EA} \quad (7)$$

Based on the above, the apparent age was estimated by a piston flow model (PFM) using the calculated SF_6 atmospheric equivalent concentration and the data on changes in atmospheric SF6 concentration over time. This model assumes that groundwater mixing does not occur until the groundwater is recharged and discharged. As the average concentration, the values published by the USGS (United States Geological Survey) from 1940 to June 2017 and the NOAA (National Oceanic and Atmospheric Administration) from June 2017 to May 2021 are used.

The age estimation method using PFM assumes that the SF_6 concentration at the time of recharge is preserved from groundwater recharge to runoff. The retention time of the sample water can be estimated by comparing it with the SF_6 concentration in the atmosphere shown by the curve. A difference in pptv was observed. Therefore, using the mean value of atmospheric SF6 concentration during the observation period in the target basin, the secular change data in the northern hemisphere was corrected by proportional allocation to create a correction curve for the target basin. Measurement results that greatly deviated from the correction curve were judged to be outliers and were excluded (Figure 9).

We used the SF_6 apparent age data to have an initial estimation of the spring water age. This initial estimation is considered as the first parameter in the model calibration and fitting process that is part of the parameter search show in the following subsections.

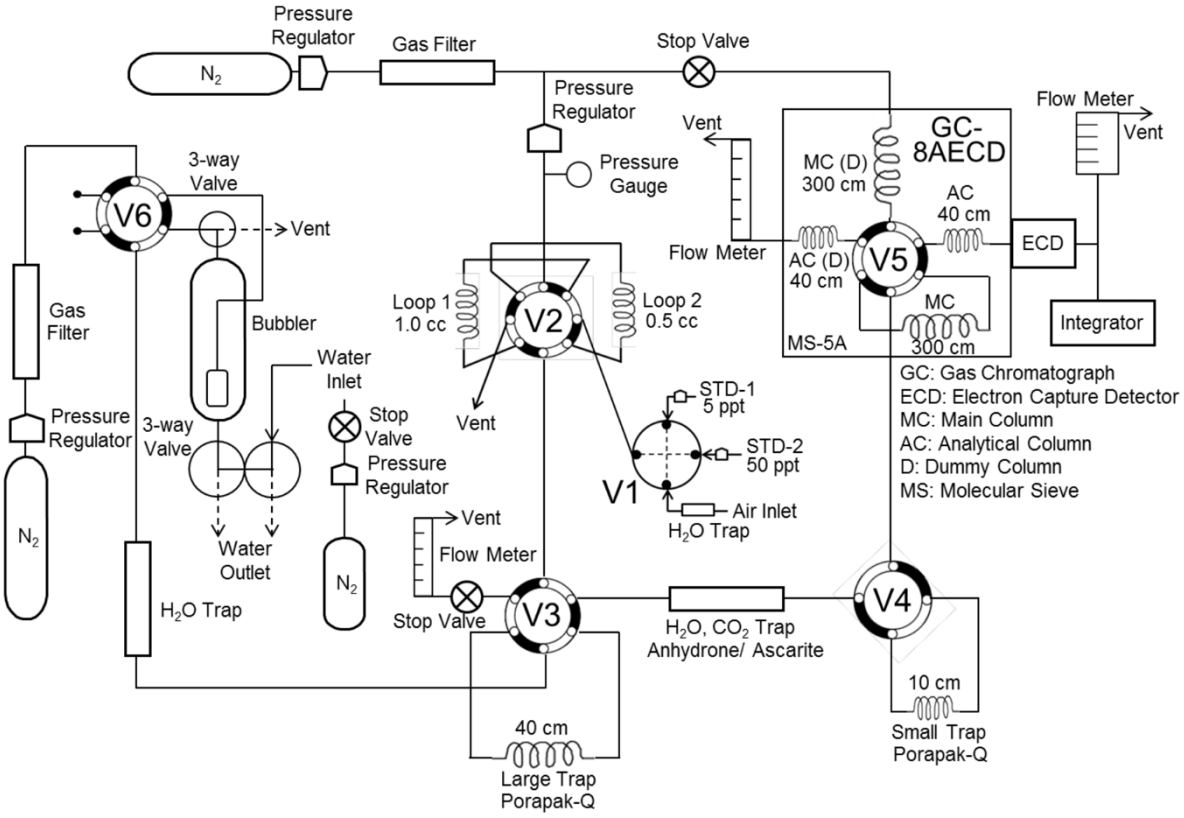

Figure 8. Overview of Dissolved Sulfur Hexafluoride Analysis System (From Sakakibara, 2018)

Table 2. Coefficient (SF_6) used to calculate the constant of proportionality (IAEA, 2006)

K_H (SF_6)	a_1	a_2	a_3	b_1	b_2	b_3
$Mol \cdot kg^{-1} \cdot (1013.25\ hPa)^{-1}$	–98.7264	142.803	38.8746	0.0268696	–0.0334407	0.0070843
$Mol \cdot L^{-1} \cdot (1013.25\ hPa)^{-1}$	–96.5975	139.883	37.8193	0.0310693	–0.0356385	0.00743254

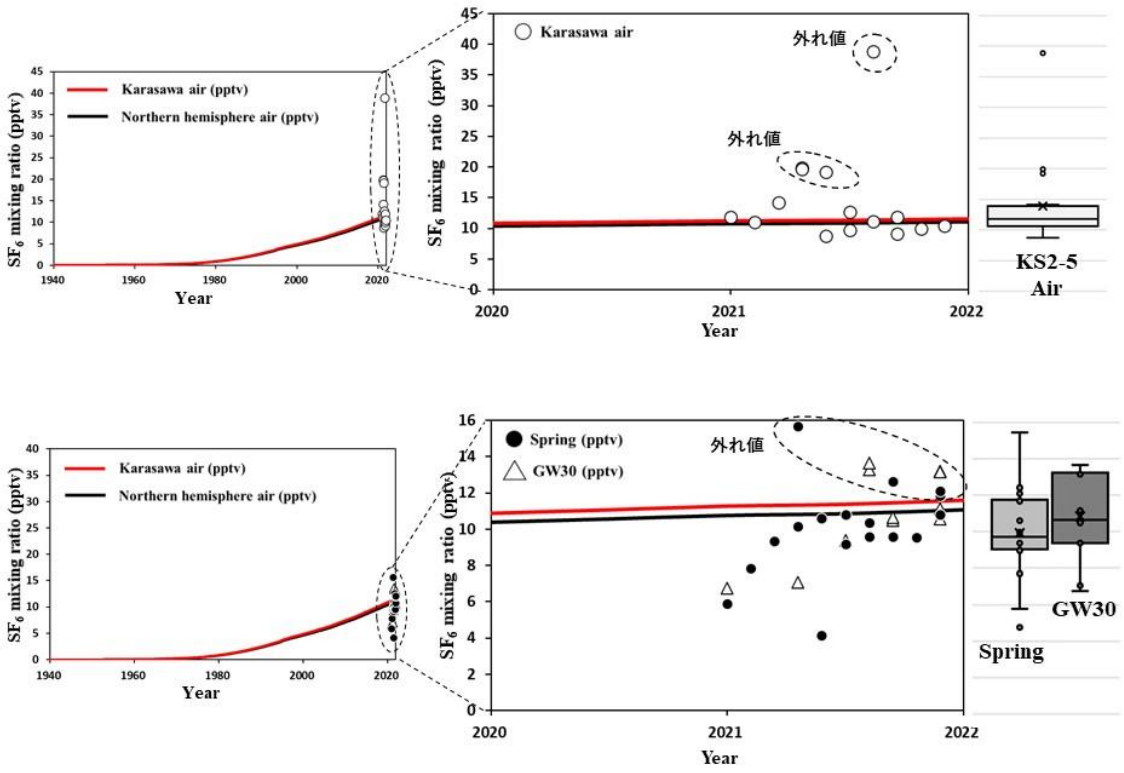

Figure 9. Annual changes in atmospheric concentration of sulfur hexafluoride (SF6) in the study area. The black straight line is the northern hemisphere mean (NOAA and USGS), and the red straight line is the proportional correction of the northern hemisphere mean. (From Suzuki, 2022)

3.3.2 SF_6 Apparent Age Analysis

We estimated the apparent ages of the spring water and groundwater samples using SF_6 concentrations according to International Atomic Energy Agency (IAEA, 2006) guidelines, and the procedure described Busenberg and Plummer, 2000. Using the SF_6 water and atmospheric data, the piston flow model (PFM) was applied to calculate the apparent ages. The atmospheric SF_6 concentrations measured in the study area differed by approximately 3–5 pptv from northern hemisphere values (Figure 10).

As we see on Figure 10, the SF_6 concentrations of 17 spring water samples collected from 2020 to 2021 were investigated. After analyzing the measured air concentrations of SF_6 in the Mount Karasawa area and those in the spring water samples, we constructed the lines shown on the figure. Since we had the SF_6 air concentrations for the corresponding spring water samples, we could obtain each sample's recharge year by comparing it to the Mount Karasawa line. Therefore, we obtained the apparent age of each sample, and the average value weighted by the discharge of the sampling day.

The PFM dating method assumes that the SF_6 concentration in the water sample at the time of recharge is preserved. This value is used to correct the atmospheric conversion. Using the average SF_6 concentration of the air in the study area during the observation period, the northern hemisphere data were proportionally distributed and corrected, and a correction line (Mt. Karasawa line) was generated.

The apparent ages of the water samples can be estimated by comparing them with the atmospheric SF_6 concentrations (indicated by the air line in Figure 10). Henry's Law was used to convert the concentrations of SF_6 dissolved in the water samples to the atmospheric concentrations at the time of recharge. Using the concurrent spring water samples and SF_6 concentrations in the air, we determined when that sample of spring water was recharged, from which we calculated the apparent age of each sample.

We used the SF_6 apparent age data to have an initial estimation of the spring water age. This

initial estimation is considered as the first parameter in the model calibration and fitting process that is part of the parameter search show in the following sections and chapters.

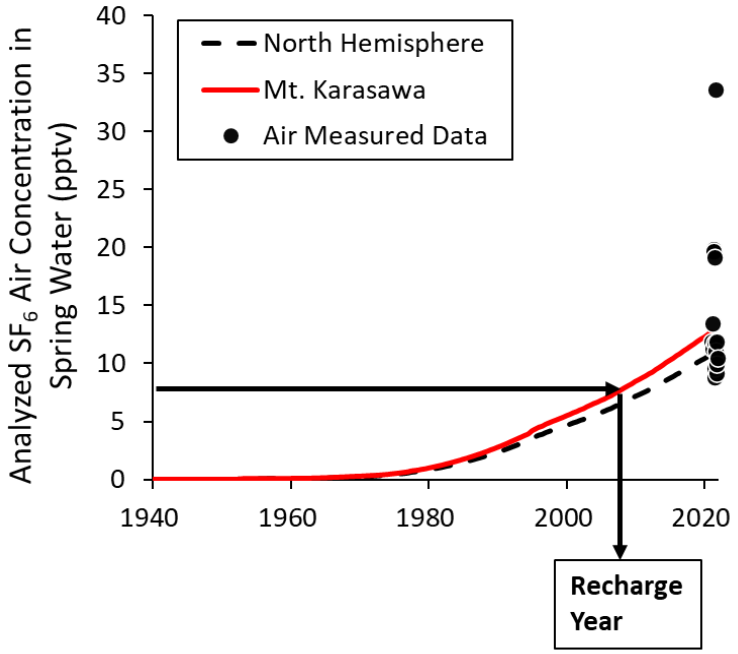

Figure 10. Air conversion lines (Mt. Karasawa area and North Hemisphere), according to the SF_6 concentrations in the air obtained in the study area, which indicate the recharge year of each water sample.

3.4 Selection of the Best Mean Transit Time (MTT) Model

In order to select the best out of different models that have been studied before, Exponential Piston-Flow Model and Dispersion Model, we evaluated the error Root Mean Square Error (RMSE), comparing their results. After analyzing these errors, we judged that for the following discussion of this study area the Exponential Piston-Flow results, especially the MTT, should be the one considered for the analytical process of this study.

According to statistical analysis, the EPM is considered to be the model that best expresses the hydrological process at the study area, and its results were used to continue this research and make a conceptual model of the groundwater volume storage.

3.5 Mean Transit Time (MTT) Estimation Model

In this study, the MTT of spring water and groundwater was induced by using the stable isotopes of hydrogen and oxygen as tracers, then estimating the d-excess variations using the Exponential-Piston Flow Model (EPM).

The d-excess of water samples expresses the close correlation between ^{18}O and ^{2}H in precipitation which can be demonstrated by the global meteoric water line, which has the general form as follows.

$$\delta D = 8 \times \delta 18O + d\,, \tag{8}$$

Where the offset d is called deuterium excess or d-excess. Since in Japan, the air masses that cause rainfall to have seasonal variations, which make them easier to target and analyze; in this study, the d-excess value is used as a tracer to analyze the state of mixing waters in the subsurface.

Maloszewski and Zuber (1982) showed that for a system with a steady flow, the output isotopic tracer is related to the input isotopic tracer by the following convolution integral:

$$\delta out(t) = \int_0^{\infty} g(t')\, \delta in(t - t')\, dt', \quad (9)$$

Where $\delta out(t)$ is the output signature, t' is the entry time into the system, t is the calendar time, δin is the input signature, and $g(t')$ is the transit time distribution. The $g(t')$ used in this study was the exponential piston flow model (EPM). This model was selected after comparing different models to best explain the characteristics of the study area (Silveira Baptista, 2020). The EPM exhibited the smallest error for each parameter and could be used to describe the study catchment.

According to Kabeya *et al*. (2007), the EPM can be expressed as:

$$g(t) = \frac{\beta}{\tau} exp\left(-\frac{\beta t}{\tau} + \beta - 1\right), \quad (10)$$

Where β is the total water volume divided by the volume with an exponential distribution of transit times, t is the calendar time, and τ is the MTT.

Since δin in Equation (9) for this study is the d-excess value of rainfall, it can be represented by the periodic seasonal variation of precipitation d-excess value and it can be approximated by the following Equation 11.

$$din\,(t) = do + Ain \sin\omega t\,, \quad (11)$$

Where din represents the δin from the convolution integral, do (‰ V-SMOW) is the weighted average of d-excess values during precipitation, Ain (‰ V-SMOW) is the annual fluctuation range of d-excess values, ω (rad/day) is the angular frequency of fluctuations.

Then, in order to estimate the mean residence time, the seasonal variation in the output d-excess becomes the following Equation 12.

$$dout\,(t) = do + B \sin(\omega t + \varphi)\,, \quad (12)$$

Where B (‰ V-SMOW) is the amplitude of the output d-excess and φ is the phase lag.

We determined the smallest possible root mean square error (RMSE) of the model to estimate the similarity of the calculated output to the observed data, as follows:

$$\mathrm{RMSE} = \sqrt{\frac{\sum_{i=1}^{n}(Oi-Xi)^2}{n}}, \quad (13)$$

where *Oi* is the *i*th observed value, *Xi* is the corresponding value calculated by the model, and *n* is the sample size.

The water transit time is equivalent to the total storage divided by the water flux (McGuire and McDonnell, 2006); therefore, we obtained the storage volume using:

$$\mathrm{MTT} = \text{Storage Volume/Flow Rate}, \quad (14)$$

where the storage volume (mm) is the amount of water stored in the catchment during each year of the study period, and the average discharge (mm/d) is the amount of runoff from the spring site, which was assumed to be an average value per year. The MTT values determined in this study are expressed in months.

3.6 Model Calibration and Fitting Process

The spring water and groundwater MTT were estimated using the SF_6 apparent age-weighted average to calibrate the EPM parameters according to the temporal variations in the d-excess of the stable isotopes.

To find the pair of parameters (β, τ) we follow the subsequent two-step method:

- The first step is to find β. We search in the range of 1 to 2, in increments of 0.01. We consider the initial τ equal to the SF_6 apparent age weighted average (From the SF_6 apparent age primary estimation). We select the β to the value with the lowest RMSE.
- Then, the second step is to find τ. We search in the range of 1 to 100, in increments of 0.1. We select τ that is associated with the lowest RMSE.

We used the R Studio, which is a software for statistical computing, to optimize the parameters search. This way, the data can be calculated automatically following the parameter search range as shown above and the best fitted ones are found. Thus, the pair of parameters (β, τ) is the one following this two-step methodology.

In order to confirm that this methodology is the most appropriate one, we compared the previous mentioned method to another one in which the parameter search was done without the SF_6 apparent age primary estimation. This other way started the parameter search randomly, and the results showed that a greater number of trials were needed and the error is still higher. This confirms that this study's methodology needs less trials during the parameter search and is the one with the lowest error.

Therefore, this study's MTT was determined following the multi-tracer methodology for each study period in which experimental investigations were conducted in the study area. The initial parameter can be found from previous data analysis and, therefore, it is an initial estimation based on theoretical knowledge, therefore likely to be correct. Since previous studies have exclusively used trial-and-error approaches, we propose that this new method provides more reliable MTT estimates.

CHAPTER 4 RESULTS

4.1 Hydrological Characteristics of the Headwater Catchment

4.1.1 Long-term Changes of Runoff and Groundwater Level

Figure 11 shows the long-term fluctuations in precipitation and runoff of the catchment stream water from April 2010 to November 2021. These fluctuations did not include substantial changes in the annual rainfall curve before or after thinning was performed. Forest thinning occurred in October 2011. The stream water runoff was relatively high in June and July (70–100 mm/d) when rainfall was also high, and was relatively low in January and February (0.001–0.5 mm/d) when precipitation decreased. This indicates that seasonal steady-state fluctuations occurred annually.

In addition, Figure 11 shows groundwater levels (GWL) measured in the two boreholes during the observation period (June 2010–November 2021). The groundwater level in the groundwater 15 m observation well was steady over time, with a slight increase soon after thinning. The groundwater level in the GW 30 m observation well exhibited wider oscillations throughout the years, including a large decrease after 2019. The GW 30 m groundwater level increased considerably under higher precipitation, but the response speed to rainfall was delayed by about 2–3 days compared to the GW 15 m observation well. The fluctuations in groundwater level were large (about 2 m); however, the response speeds of the observation wells to rainfall differed. When compared to the stream runoff, we found that the increasing flow rate exhibited a similar tendency as the increases in groundwater level.

The annual water balance at the Mount Karasawa study area can be understood through Table 3, which shows the annual amounts of precipitation (P), stream discharge (Q) and water

loss (L, considering that L = P - Q) in mm per year, from 2010 to 2021. The years 2018 and 2019 have no discharge data due to strong typhoon events in those years that have made the data unable to be calculated properly.

As we can see in the table, the precipitation trend is stable throughout the years. The stream water discharge shows an increasing trend on the years soon after thinning. On the years long after thinning, especially from 2016, the stream water discharge shows a decreasing trend.

The water loss, in which evapotranspiration is a part of it, shows a decreasing trend on the years soon after thinning. On the years long after thinning, especially from 2016, the water loss shows an increasing trend.

Table 4 shows the monthly stream runoff and precipitation in mm during all the observation period since 2010. There is no significant change in the annual rainfall condition curve before and after thinning, which shows that there is no significant difference in the magnitude and frequency of annual rainfall events. The flow rate of spring water is relatively high in June and July when rainfall is also increased, and is relatively low in January when there is a decrease in precipitation, which shows a seasonal fluctuation.

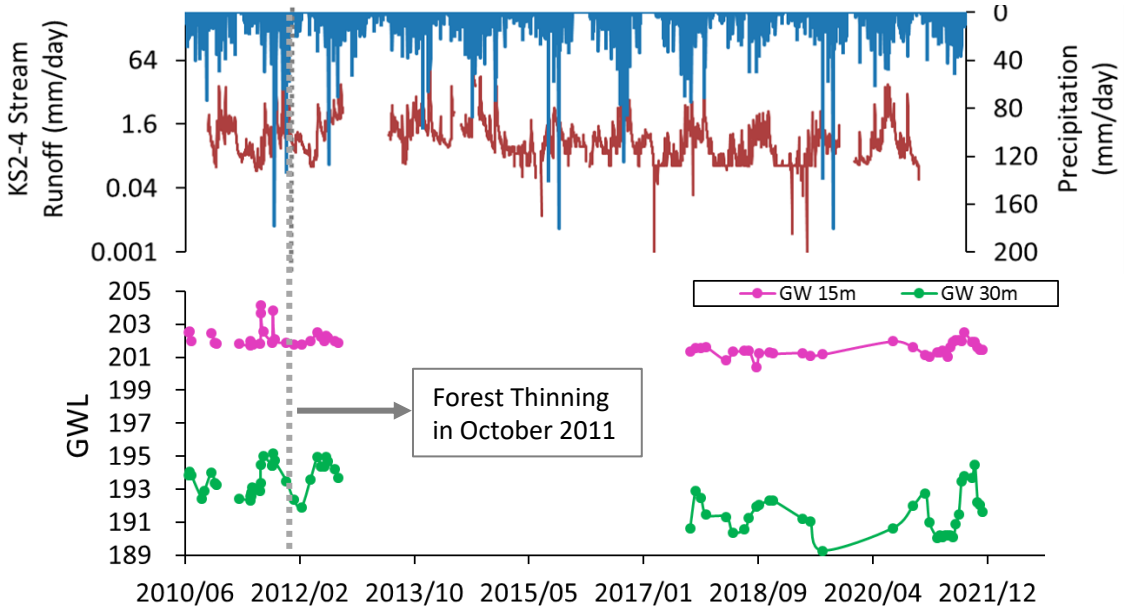

Figure 11. Stream water precipitation and runoff measurements, groundwater (GW) levels measured in the two boreholes, during the observation period (June 2010–November 2021). The forest was 50% thinned in October 2011.

Table 3. Annual water balance at the Mount Karasawa study area.

Year	Precipitation (mm)	Discharge (mm)	Water Loss (mm)
2010	1197.9	241.9	955.9
2011	1411.0	726.6	684.4
2012	1295.2	495.6	799.6
2013	1207.8	759.5	448.3
2014	1419.8	923.4	496.3
2015	1342.2	843.3	498.9
2016	1434.3	390.6	1043.7
2017	1322.8	341.2	981.6
2018	979.9	-	-
2019	1291.2	-	-
2020	1092.2	261.6	830.6
2021	1189.6	328.7	860.9

Table 4. Annual Precipitation (P, in mm), Stream Runoff (R, in mm) and Runoff Ratio at the Mount Karasawa study area.

		Jan.	Feb.	Mar.	Apr	May	Jun.	Jul.	Aug.	Sep.	Oct.	Nov.	Dec.	Total
2010	P	--	--	--	--	--	--	--	81.6	216.6	118.4	86.0	85.8	588.4
	R	--	--	--	--	--	--	--	27.7	44.9	56.9	71.3	41.2	241.9
	Ratio	--	--	--	--	--	--	--	0.3	0.2	0.5	0.8	0.5	0.4
2011	P	0.2	59.6	47.0	30.2	154.4	77.0	410.4	342.6	342.6	94.0	50.4	26.8	1635.2
	R	8.9	8.8	11.2	5.3	22.9	32.1	314.3	211.9	211.9	33.6	19.0	16.0	895.9
	Ratio	44.6	0.1	0.2	0.2	0.1	0.4	0.8	0.6	0.6	0.4	0.4	0.6	0.5
2012	P	32.2	35.6	111.4	97.2	281.8	165.0	177.6	43.2	190.6	76.2	51.6	32.8	1295.2
	R	8.6	6.0	62.6	41.9	154.4	132.7	89.5	40.8	68.1	29.2	25.9	9.5	669.1
	Ratio	0.3	0.2	0.6	0.4	0.5	0.8	0.5	0.9	0.4	0.4	0.5	0.3	0.5
2013	P	25.6	25.8	24.4	139.8	74.2	105.4	130.6	143.0	205.6	254.6	28.4	50.4	1207.8
	R	0.2	2.7	11.4	55.9	31.5	21.8	54.8	80.5	232.9	216.5	29.9	24.3	762.4
	Ratio	0.0	0.1	0.5	0.4	0.4	0.2	0.4	0.6	1.1	0.9	1.1	0.5	0.6
2014	P	11.6	37.4	56.2	79.4	84.2	371.4	230.4	132.4	77.0	253.4	60.0	26.4	1419.8
	R	16.2	88.8	3.2	23.5	39.8	358.8	146.1	44.2	26.3	149.5	14.6	12.5	923.5
	Ratio	1.4	2.4	0.1	0.3	0.5	1.0	0.6	0.3	0.3	0.6	0.2	0.5	0.7
2015	P	31.6	34.0	62.0	91.8	55.6	154.8	235.4	136.0	324.6	51.6	134.3	30.5	1342.2
	R	10.9	9.0	17.0	45.5	11.0	21.1	325.3	108.8	223.9	17.8	32.9	20.1	843.3
	Ratio	0.3	0.3	0.3	0.5	0.2	0.1	1.4	0.8	0.7	0.3	0.2	0.7	0.6
2016	P	57.5	33.0	70.0	96.2	86.0	130.4	121.8	388.8	270.0	49.4	87.2	44.0	1434.3
	R	15.1	2.3	18.8	21.5	10.4	17.1	25.5	168.2	64.4	14.4	11.0	21.9	390.6
	Ratio	0.3	0.1	0.3	0.2	0.1	0.1	0.2	0.4	0.2	0.3	0.1	0.5	0.3
2017	P	23.5	9.8	71.2	71.2	76.2	104.0	230.2	227.2	149.8	327.2	22.6	9.9	1322.8
	R	14.6	3.3	7.1	11.6	6.2	7.9	35.0	100.2	27.2	99.4	21.8	6.8	341.2
	Ratio	0.6	0.3	0.1	0.2	0.1	0.1	0.2	0.4	0.2	0.3	1.0	0.7	0.3
2020	P	62.8	20.4	85.8	142.6	103.6	190.2	216.0	32.6	96.2	131.2	10.8	0.1	1092.3
	R	7.6	6.8	8.6	42.4	23.4	29.1	76.5	22.8	7.9	26.0	7.6	3.0	261.6
	Ratio	0.1	0.3	0.1	0.3	0.2	0.2	0.4	0.7	0.1	0.2	0.7	30.4	0.2
2021	P	17.4	39.4	100.0	71.2	91.0	180.2	264.2	172.0	75.0	78.4	27.0	73.8	1189.6
	R	2.4	3.1	6.3	5.3	4.6	32.0	130.4	91.3	19.9	12.9	5.6	14.8	328.7
	Ratio	0.1	0.1	0.1	0.1	0.1	0.2	0.5	0.5	0.3	0.2	0.2	0.2	0.3

4.1.2 Stable Isotopes of Water Variation in Precipitation, Groundwater and Spring Water

The oxygen isotope ratios ($\delta^{18}O$ ‰) and hydrogen isotope ratios ($\delta^{2}H$ ‰) distribution in spring water (KS25-SP), groundwater (GW 15 m) and groundwater (GW 30 m) Before Thinning, Soon After Thinning and Long After Thinning can be seen on Figures 12 and 13. The oxygen isotope ratio of spring water and both groundwater observation wells show an upward tendency Soon After Thinning, which slightly decreases Long After Thinning.

Figure 14 shows the spring water, groundwater and precipitation d-excess values from June 2010 to November 2021. The d-excess minimum, maximum and average values of precipitation, spring water (KS25-SP), groundwater (GW 15 m) and groundwater (GW 30 m), including the stream water, Before Thinning, Soon After Thinning and Long After Thinning can be seen on Tables 5, 6, 7, 8 and 9. The fluctuations in the precipitation d-excess were large, for example (-1.3 – 18.9‰) Before Thinning, owing to the seasonal rainfall variations in the study area. In contrast, the spring water d-excess fluctuated less widely, for example (10.9 – 11.9‰) Before Thinning.

The d-excess ratio of precipitation was -1.3 ‰ to 18.9 ‰ Before Thinning, 7.2 ‰ to 23.8‰ Soon After Thinning, and 1.4 ‰ to 25.5 ‰ Long After Thinning. The d-excess ratio of spring water and both groundwater observation wells show an and increase on their values Soon After Thinning and then, a subsequent decrease Long After Thinning.

In addition to the rainfall effect, the increase in the d-excess value in the precipitation water can be explained because the local evaporated water selectively evaporates from water molecules containing lighter isotopes. Hence, if we observe both distributions in precipitation, spring water and groundwater, the ratio of d-excess is lower in the periods Before Thinning and Long After Thinning. We can understand that for this area, evapotranspiration processes contribute to the change of stable isotopes in the precipitation.

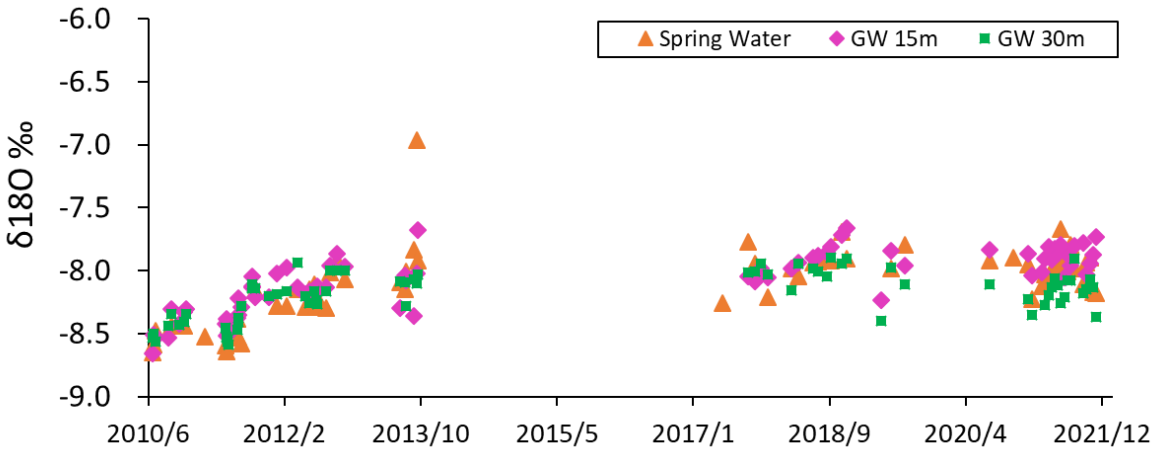

Figure 12. Long-term variations in spring water and groundwater stable isotopes of oxygen-18 (δ18O‰) during the observation period (June 2010–November 2021).

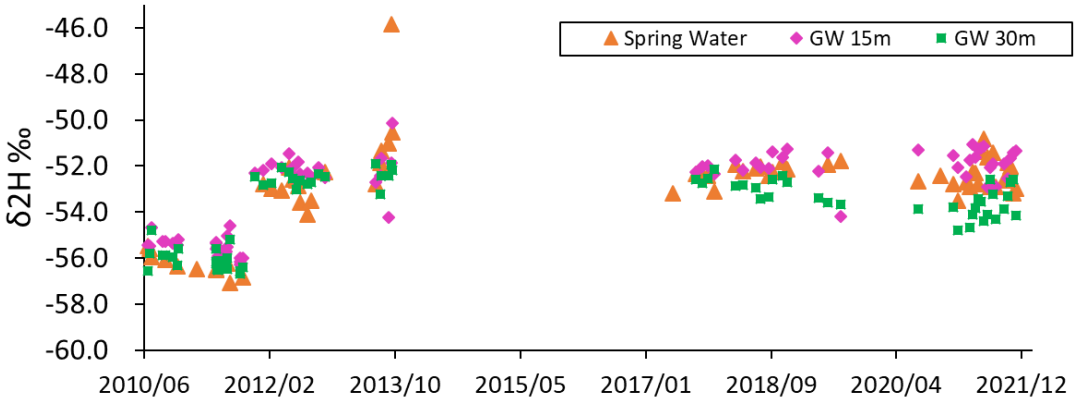

Figure 13. Long-term variations in spring water and groundwater stable isotopes of deuterium (δ^2H‰) during the observation period (June 2010–November 2021).

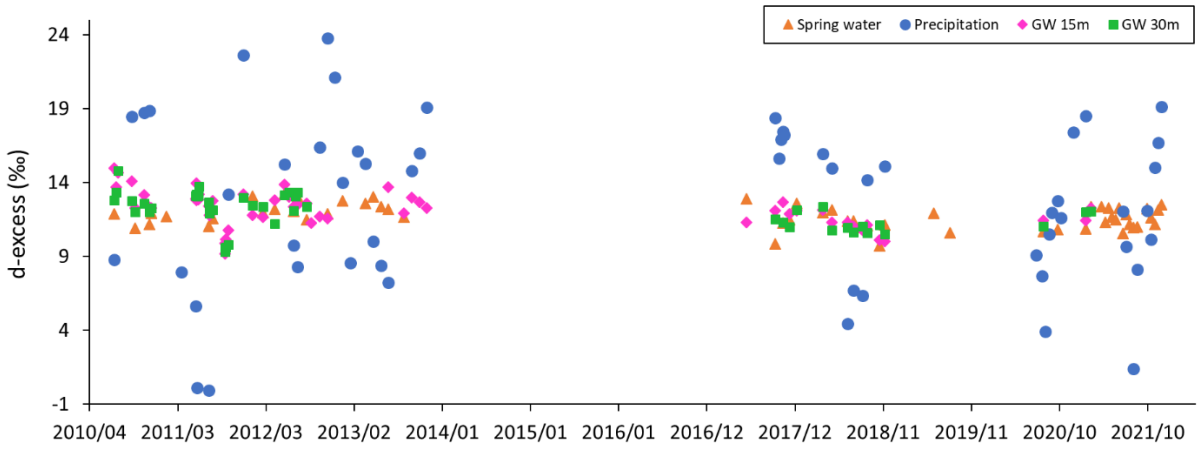

Figure 14. Long-term variations in precipitation, spring water and groundwater d-excess of stable isotopes during the observation period (June 2010–November 2021).

Table 5. Observed d-excess (‰) distribution in precipitation Before Thinning, Soon After Thinning and Long After Thinning.

Observed Precipitation d-excess (‰)	Before Thinning	Soon After Thinning	Long After Thinning
Minimum	-1.3	7.2	1.4
Maximum	18.9	23.8	25.5
Average	9.03	14.1	12.2

Table 6. Observed d-excess (‰) distribution in spring water Before Thinning, Soon After Thinning and Long After Thinning.

Observed Spring Water d-excess (‰)	Before Thinning	Soon After Thinning	Long After Thinning
Minimum	10.9	11.5	9.7
Maximum	11.9	13.2	12.6
Average	11.4	12.4	11.4

Table 7. Observed d-excess (‰) distribution in groundwater at 15m deep Before Thinning, Soon After Thinning and Long After Thinning.

Observed GW 15m d-excess (‰)	Before Thinning	Soon After Thinning	Long After Thinning
Minimum	8.1	11.3	9.5
Maximum	13.9	14.0	13.6
Average	11.4	12.5	11.4

Table 8. Observed d-excess (‰) distribution in groundwater at 30m deep Before Thinning, Soon After Thinning and Long After Thinning.

Observed GW 30m d-excess (‰)	Before Thinning	Soon After Thinning	Long After Thinning
Minimum	8.2	10.9	8.9
Maximum	13.7	13.8	13.8
Average	11.1	12.5	11.4

Table 9. Observed d-excess (‰) distribution in stream water Before Thinning, Soon After Thinning and Long After Thinning.

Observed GW 30m d-excess (‰)	Before Thinning	Soon After Thinning	Long After Thinning
Minimum	-	-	10.0
Maximum	-	-	13.3
Average	-	-	11.8

4.2 SF_6 Apparent Age and the Weighted Average

Figure 15 shows the results of SF_6 concentration analysis of spring water and groundwater from a 30 m depth observation well from November 2020 to November 2021. As a general trend, the dissolved concentrations in spring water and groundwater also gradually increased. Based on these measurement results, we estimated the retention time of the spring water and the groundwater of the observation well at a depth of 30 m. 1 to 21 years for spring water, and 1 to 13.5 years for observation wells at a depth of 30 m. Springs were estimated to have a residence time of more than 10 years from November to March 2020, and less than 10 years from April to October. In the groundwater of the 30 m depth observation well, the retention time was estimated to be more than 10 years from January to April 2021 and less than 10 years from June to November 2021.

As we have seen on previously, the SF_6 apparent ages of 17 spring water collected from 2020 to 2021. After analyzing the measured air concentrations of SF_6 in the Mount Karasawa area and those in the spring water samples, we constructed the lines shown on the figure. Since we had the SF_6 air concentrations for the corresponding spring water samples, we could obtain each sample's recharge year by comparing it to the Mount Karasawa line. Therefore, we obtained the apparent age of each sample, and the average value weighted by the discharge when sampled was measured.

Tables 10 and 11 shows the apparent age of each sample and the spring water daily discharge of their sampling days. The samples (apparent age) are weighted to better match the population "weights" (daily discharge), so every term has a corresponding weight. The weighted average considers the correlation of spring water apparent age and its discharge. Hence, each sample of spring water from a specific field survey day is associated to the daily discharge of spring water on that same day. This average of the apparent age is an initial

estimation based on theoretical knowledge and is part of the parameter search and fitting process. Finally, there is one SF_6 apparent age that can be considered as the initial τ of the model parameter calibration and fitting process.

Kashiwa (2019), who used SF_6 as a tracer and estimated the apparent age of spring water and groundwater of an observation well at a depth of 30 m using the same method as in the present study, estimated the retention time of spring water at a maximum of 11 years and that of an observation well at a depth of 30 m and a maximum of 10.4 years was estimated. In particular, when water was sampled during or immediately after the occurrence of a rainfall event, the retention time of spring water was significantly longer than that during base runoff. In that case, the spring water fluctuated from less than 1 year to 7.0 years during base runoff, while fluctuated from 5.2 years to 10.9 years during rainfall events. At the time of base runoff, the fluctuations ranged from 1.9 to 2.8 years, and the residence time during rainfall events fluctuated from 8.4 to 10.4 years.

However, although we did not sample water during rainfall events in this study, both the spring water sampled from November 2020 to March 2021 and the 30m depth observation well showed better results than previous studies. The maximum apparent age was estimated to be over 10 years. It is thought that this may have been due to the possibility of capturing trends in the retention time of springs and groundwater from January to March.

In IAEA (2006) and Sakakibara *et al*., 2018, has been pointed out that when targeting groundwater assumed to be relatively young, the actual apparent age where mixing occurs and the residence time estimated as the apparent age may not differ greatly. The apparent age of the spring water estimated by SF_6 was about 10.5 years. The fact that the average residence times were similar is thought to reflect the results of the reasonable estimation of residence times by both tracers.

Considering the spring water discharge, the weighted average of the apparent age of the

spring water and groundwater (GW30) samples was 39.1 and 33.5 months respectively, which was the initial estimation used for parameter calibration (τ). As described later, this result was close to the MTT from the “before thinning” and “long after thinning” periods.

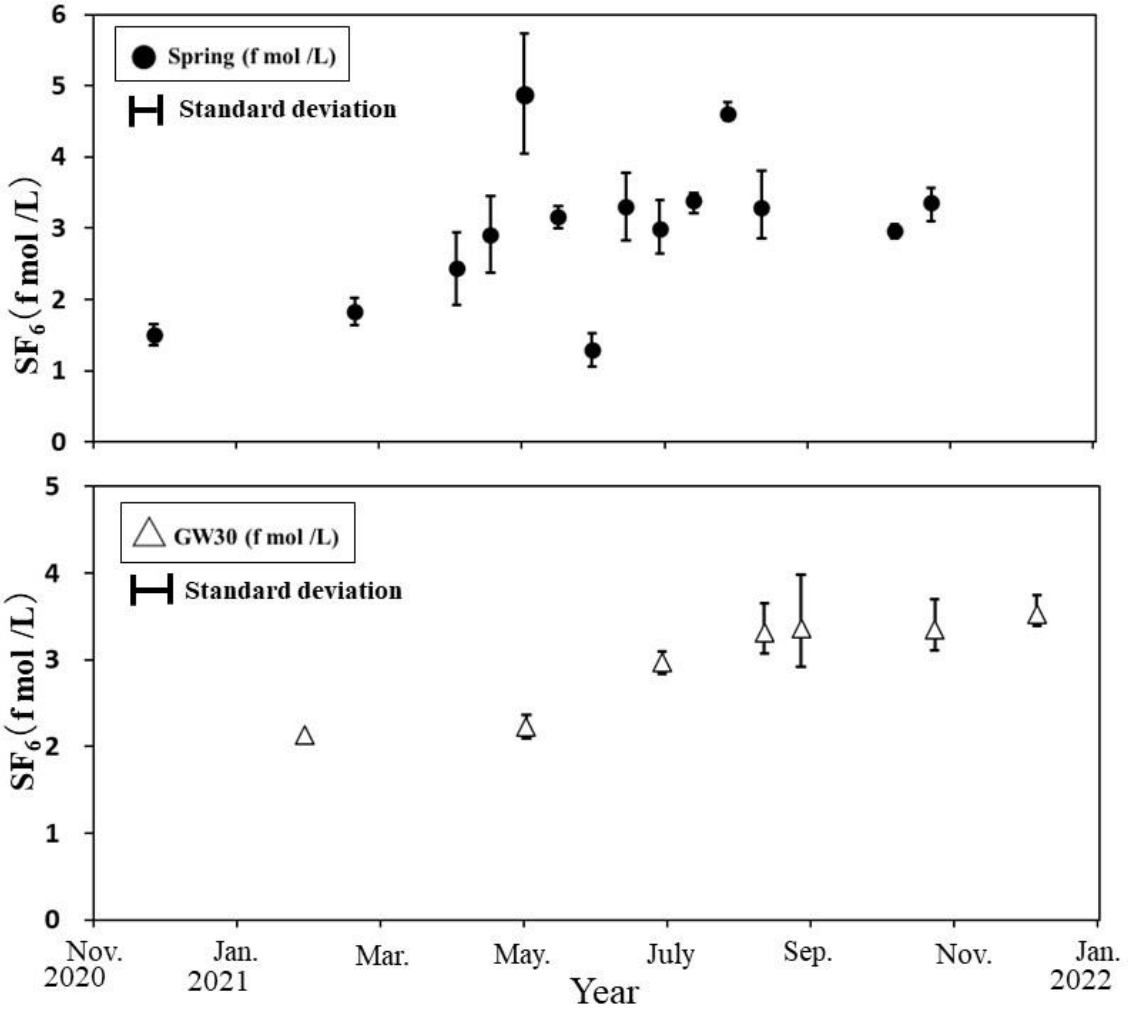

Figure 15. Concentration of sulfur hexafluoride (SF_6) in spring water and groundwater

Concentrations before atmospheric conversion are shown (From Suzuki, 2022).

Table 10. Sampling dates, apparent SF_6 age of each sample (in months) and their daily discharges (in mm/day). The weighted average of the apparent ages is 39.1 months.

Date (y/m/d)	SF_6 Apparent Age (months)	Discharge (mm/day)
2020/11/26	252	0.12
2021/2/17	204	0.10
2021/3/31	126	0.11
2021/4/14	66	0.09
2021/5/12	42	0.05
2021/5/26	78	0.06
2021/6/9	78	1.02
2021/6/23	60	0.74
2021/7/7	24	0.97
2021/7/21	36	0.11
2021/8/4	66	0.14
2021/8/19	6	2.55
2021/9/28	66	0.27
2021/10/13	30	0.34
2021/10/28	6	0.22
2021/11/10	6	0.30
2021/11/24	6	0.09

Table 11. Sampling dates, apparent SF6 age of each sample (in months) and their daily discharges (in mm/day). The weighted average of the apparent ages is 33.51 months.

Date	SF_6 Apparent Age (months)	Discharge (mm/day)
2021/1/27	162	0.10
2021/4/28	150	0.09
2021/6/23	60	0.74
2021/8/4	30	0.14
2021/8/19	24	2.55
2021/10/13	30	0.34
2021/10/28	6	0.22
2021/11/10	6	0.30
2021/11/24	12	0.09

4.3 Isotopic Content in Precipitation

The d-excess value during rainfall in the Kanto region of Japan is high in winter and low in summer. Although it can have seasonal variations, it may have extremely low values from summer to autumn due to typhoons, but in the long term it is considered that it has the same fluctuation range as usual. In this study, the d-excess value for each month is the observed value at each sampling point. And the average of the fluctuations when the observations of the entire period (from 2010 to 2021) were taken as the typical seasonal fluctuations in the study area catchment. As a result, the Ain was 13.42‰, and the average following the sine curve was 12.35‰ and ω was 0.52, which can be seen in the following equation.

$$d_{in}(t) = 12.35 + 13.42 \sin(0.52t) \quad (15)$$

4.4 Spring Water and Groundwater Mean Transit Time

The Mean Transit Time of spring water, stream water and groundwater was estimated using the Exponential Piston-Flow Model (EPM) on the three different time periods: Before Thinning, After Thinning and Long After Thinning. The d-excess values for Spring Water, Groundwater at 15m deep (GW 15 m) and Groundwater at 30m deep (GW 30 m) for each month were obtained by the observed values of stable isotopes at each sampling point on a monthly basis.

We estimated the spring water MTT using the EPM, as shown in before. The d-excess of the observed precipitation data, which was included in the model as the input content, and its fitted sinusoidal line is also shown in the Figures 16, 17 and 18. The d-excess of the spring water, groundwater 15 m and 30 m and stream water were plotted for each study period. After calibrating the model parameters and obtaining the smallest RMSE, we fit the calculated d-excess values to the observed data. The d-excess calculated using the model and the observed data exhibited long-term sinusoidal variations (Figures 19 to 28). The monthly spring water d-

excess values were obtained from the stable isotope data at each sampling point. The final EPM parameters are shown in the Table 12, for each water type and study period, “before thinning”, “soon after thinning” and “long after thinning”.

According to the τ results from the model, the MTT increased in the 2 years after forest thinning was performed. Then, 4 to 8 years later, the MTT decreased again, even if slightly for the groundwater. From June 2010 to September 2011 (before thinning), the spring water MTT was 41 months. After 50% thinning was performed in October 2011, the MTT was 55 months from November 2011 to December 2013 (soon after thinning). We understand that with a higher infiltration soon after thinning, older groundwater mixed with the younger one and was pushed out of the underground system.

In addition, six years after thinning, the spring water MTT was 40 months from September 2017 to November 2021 (long after thinning). The MTT during the final study period was close to the SF_6 apparent age. The lowest RMSE was 0.45 in the “soon after thinning” period. Also, we can confirm the spring water MTT by comparing it to the stream water MTT, which was 41 in the Long After Thinning period, so it is quite similar to the spring.

From June 2010 to September 2011 (before thinning), the GW 15m MTT was 38 months. After 50% thinning was performed in October 2011, the MTT was 67 months from November 2011 to December 2013 (soon after thinning). We understand that with a higher infiltration soon after thinning, older groundwater mixed with the younger one and was pushed out of the underground system. In addition, six years after thinning, the MTT was 64 months from September 2017 to November 2021 (long after thinning). The lowest RMSE was 0.62 in the “soon after thinning” period.

From June 2010 to September 2011 (before thinning), the GW 30m MTT was 34 months. After 50% thinning was performed in October 2011, the MTT was 62 months from November 2011 to December 2013 (soon after thinning). We understand that with a higher infiltration soon

after thinning, older groundwater mixed with the younger one and was pushed out of the underground system. In addition, six years after thinning, the MTT was 59 months from September 2017 to November 2021 (long after thinning). The lowest RMSE was 0.78 in the "soon after thinning" period.

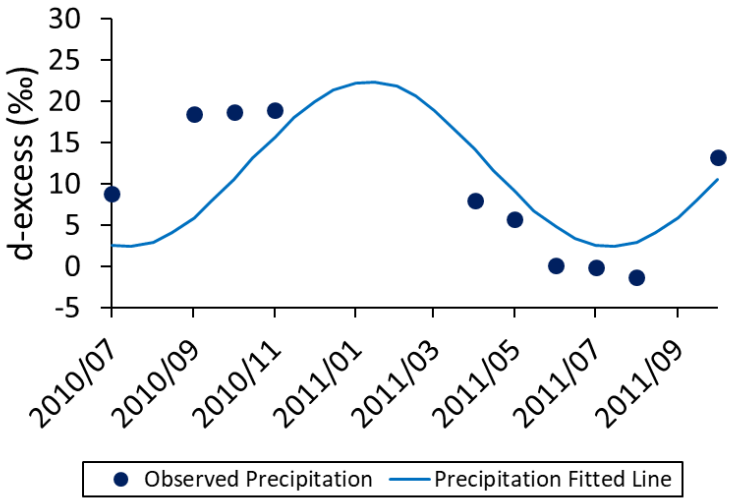

Figure 16. Precipitation d-excess and fitted line Before Thinning.

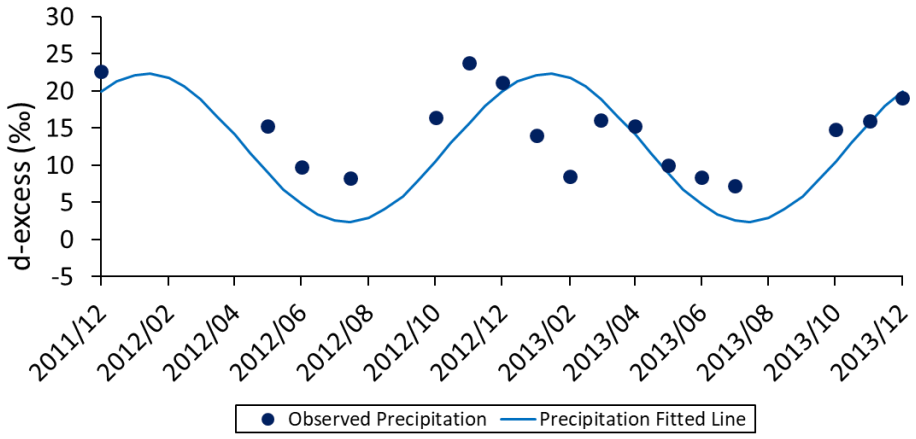

Figure 17. Precipitation d-excess and fitted line Soon After Thinning.

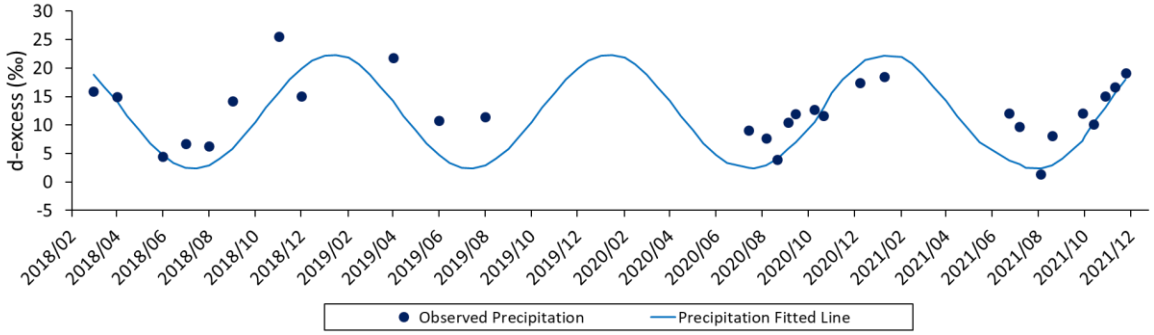

Figure 18. Precipitation d-excess and fitted line Long After Thinning.

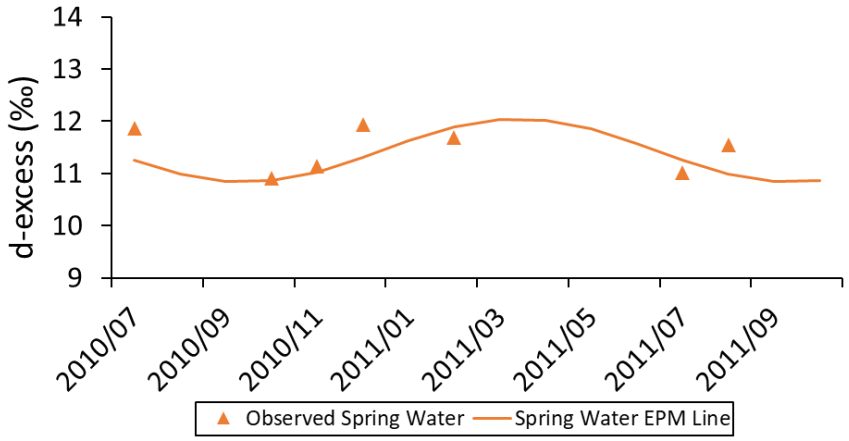

Figure 19. Variations in the spring water d-excess and MTT analysis flow applying the EPM to fit the observed data Before Thinning.

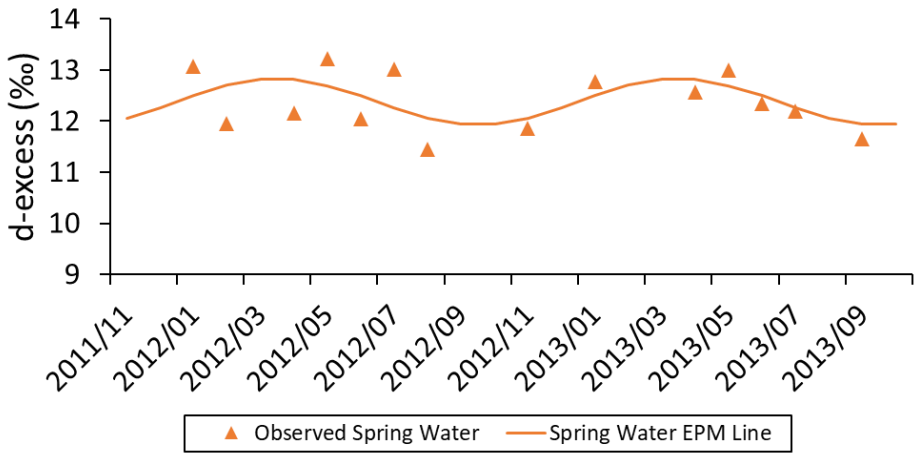

Figure 20. Long-term variations in the spring water d-excess and MTT analysis flow applying the EPM to fit the observed data Soon After Thinning.

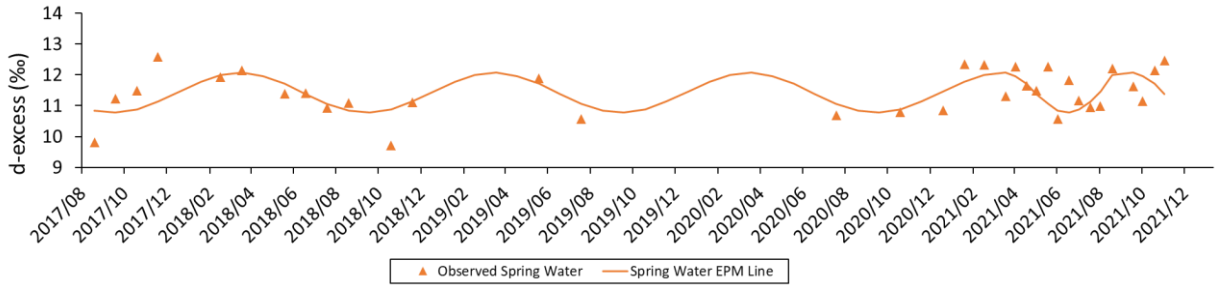

Figure 21. Long-term variations in the spring water d-excess and MTT analysis flow applying the EPM to fit the observed data Long After Thinning.

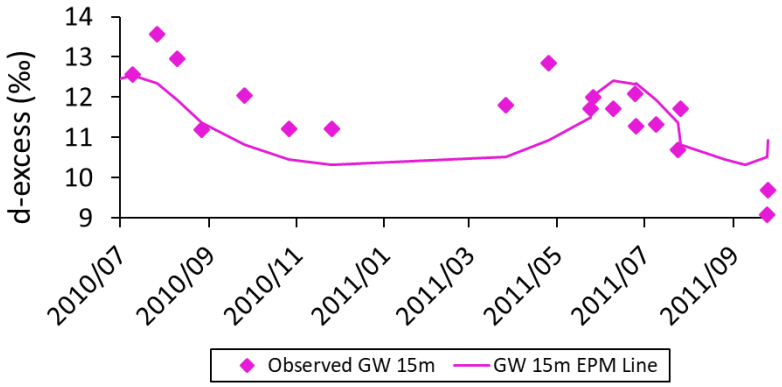

Figure 22. Variations in the groundwater 15 m d-excess and MTT analysis flow applying the EPM to fit the observed data Before Thinning.

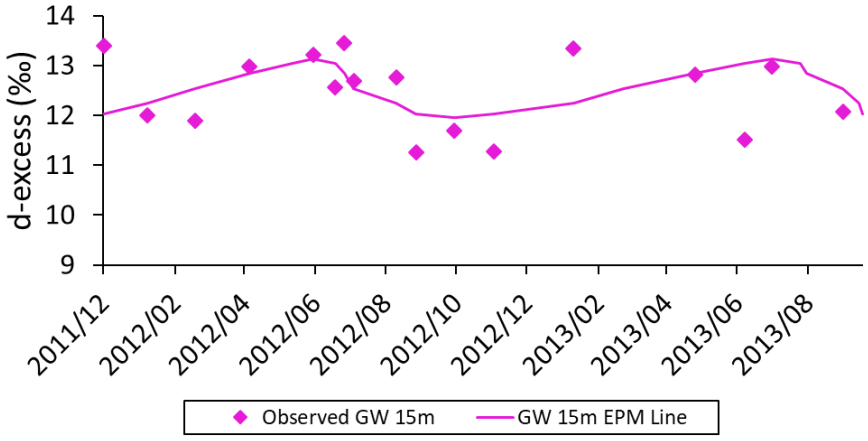

Figure 23. Variations in the groundwater 15 m d-excess and MTT analysis flow applying the EPM to fit the observed data Soon After Thinning.

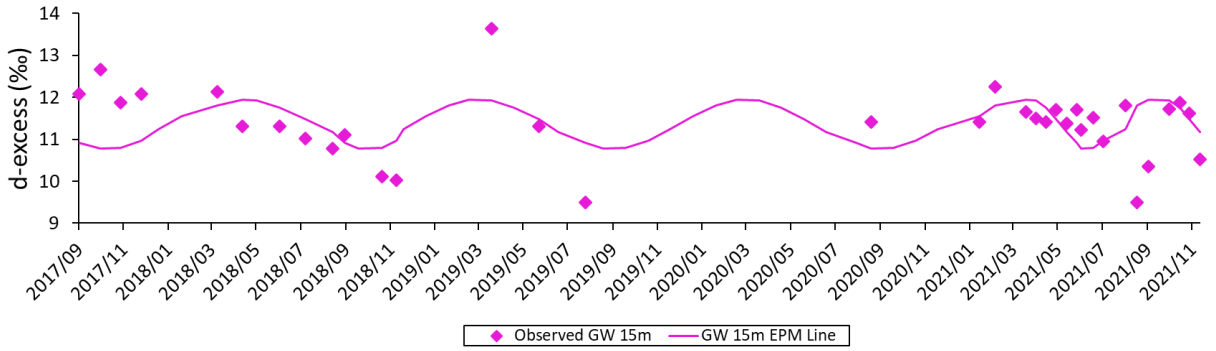

Figure 24. Variations in the groundwater 15 m d-excess and MTT analysis flow applying the EPM to fit the observed data Long After Thinning.

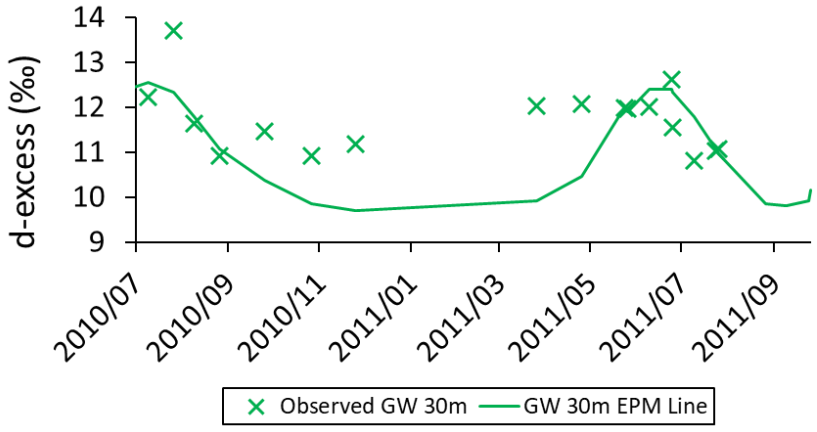

Figure 25. Variations in the groundwater 30 m d-excess and MTT analysis flow applying the EPM to fit the observed data Before Thinning.

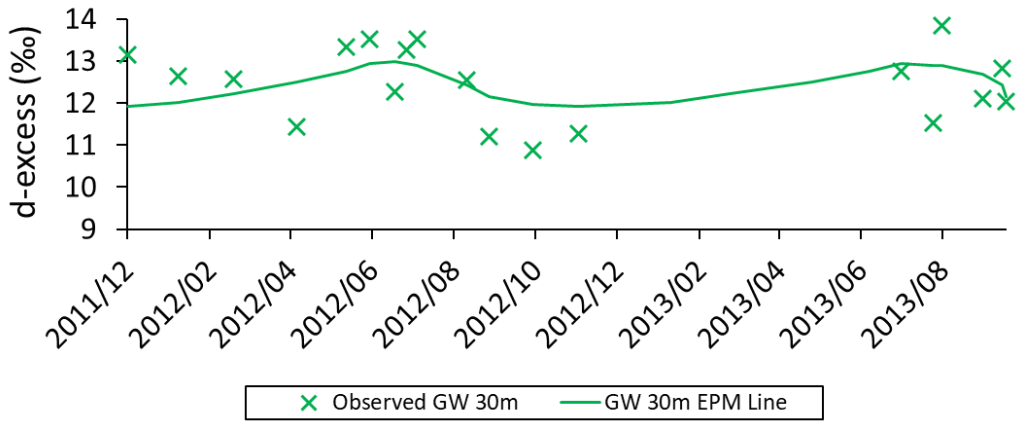

Figure 26. Variations in the groundwater 30 m d-excess and MTT analysis flow applying the EPM to fit the observed data Soon After Thinning.

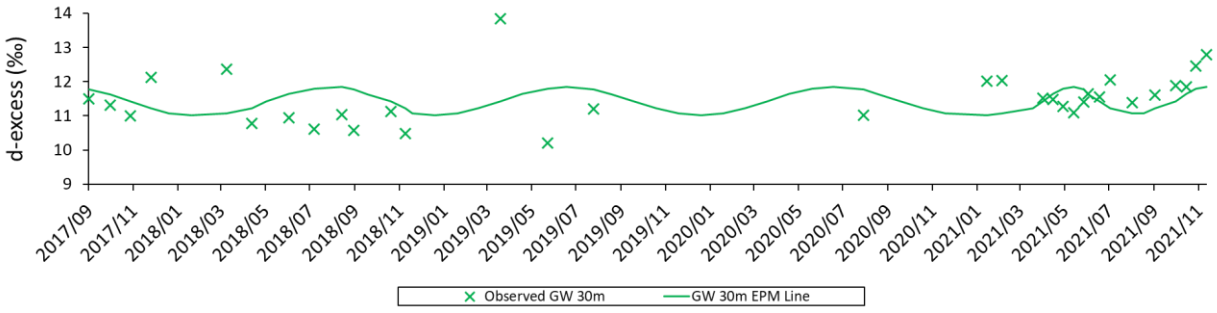

Figure 27. Variations in the groundwater 30 m d-excess and MTT analysis flow applying the EPM to fit the observed data Long After Thinning.

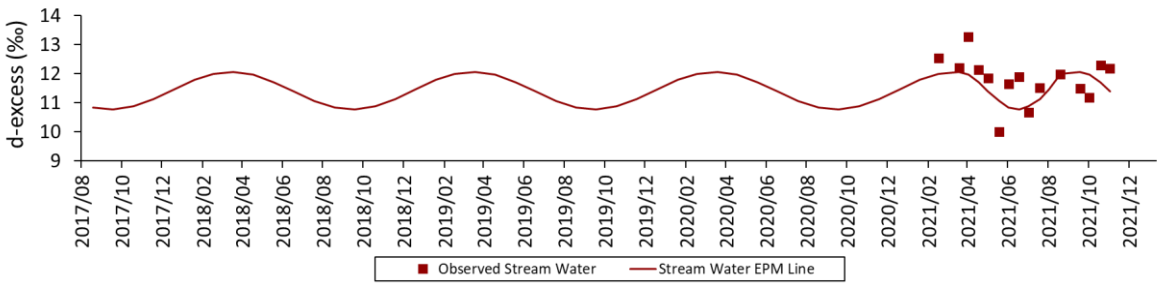

Figure 28. Variations in the stream water d-excess and MTT analysis flow applying the EPM to fit the observed data Long After Thinning.

Table 12. Final parameters of the EPM after the fitting process, for each water sampled and study period. The MTT is represented by the τ parameter in months. The precipitation input function is $din(t) = 12.35 + 13.42 \sin(0.52t)$.

		Before Thinning	Soon After Thinning	Long After Thinning
Spring Water	τ (months)	41	55	40
	β	1.26	1.01	1.34
	RMSE	0.47	0.46	0.64
Groundwater 15 m	τ (months)	38	67	64
	β	1.7	1.6	1.5
	RMSE	0.86	0.62	0.87
Groundwater 30 m	τ (months)	34	62	59
	β	1.8	1.3	1.4
	RMSE	0.87	0.78	0.85
Stream Water	τ (months)	-	-	41
	β	-	-	1.3
	RMSE	-	-	0.7

4.5 Long-term Hydrological Processes at the Study Area

Based on the MTT and the average annual spring water discharge, we determined the storage volume of the catchment over time. As shown in Figure 29, the average volume of the catchment increased from 676 mm to 1,171 mm 1–2 years after the forest was thinned. Approximately six years later, the storage volume was decreased to 588 mm.

In the proposed schematic model of the study area (Figure 29), considering stable precipitation over time and the water balance analysis of the study area, changes in groundwater storage are explained by differences in the MTT and fluctuations in water loss and infiltration. Soon after the forest was thinned, infiltration and groundwater storage increased, while water loss decreased. During the years long after thinning, the opposite trend was observed.

The water balance at the Mount Karasawa study area can be understood through Table 3, which shows the annual amounts of precipitation (P), stream discharge (Q) and water loss (L) in mm per year, from 2010 to 2021. The water loss is taking into consideration the analysis from (Chiu *et al*., 2022), in which the estimated L = P - Q. The years 2018 and 2019 have no discharge data due to strong typhoon events in those years that have made the data unable to be calculated properly.

Changes in vegetation cover could also have occurred in the catchment throughout the study period. Such variations may be associated with an understory vegetation post-recovery phase, as forest thinning had occurred several years prior. Therefore, we suggest that future studies should include information on vegetation cover recovery in addition to hydrological data. Consequently, we stress that the effects of forest thinning on hydrological processes in small headwater catchments are extensive. The impacts caused by thinning were observed soon after thinning occurred because of the MTT, followed by increases in storage volume during the following 2 years. In contrast, six years after thinning, the impacts were smaller and

hydrological processes returned to their original status trend, as demonstrated by the lower MTT and storage volume values.

The precipitation trend is stable throughout the years. The stream water discharge shows an increasing trend on the years soon after thinning. On the years long after thinning, especially from 2016, the stream water discharge shows a decreasing trend. The water loss, in which evapotranspiration is a part of it, shows a decreasing trend on the years soon after thinning. On the years long after thinning, especially from 2016, the water loss shows an increasing trend.

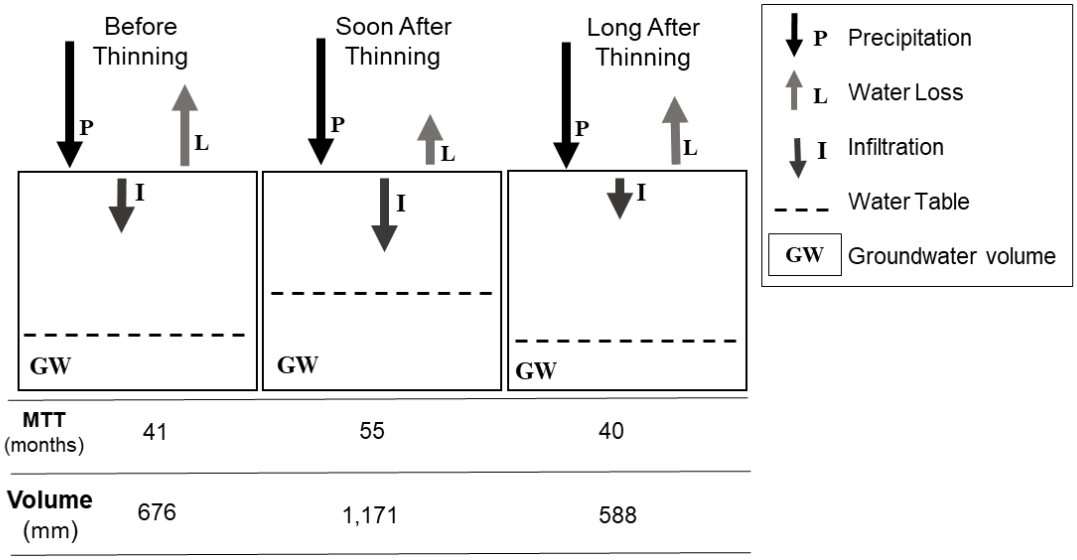

Figure 29. Schematic diagram illustrating hydrological processes in the study area during the "before thinning" (2010–2011), "soon after thinning" (2011–2013), and "long after thinning" (2017–2021) study periods. Arrow lengths demonstrate changes in the amount of water loss and infiltration, with the precipitation arrow remaining stable. The water table line indicates fluctuations in groundwater storage. The MTT and volume are shown below the diagram.

CHAPTER 5 DISCUSSION

This study aimed to determine how the characteristics of a forest alter short and long-term hydrological processes in a small forested headwater catchment, considering a new multi-tracer methodology. Previous studies (Jung *et al*., 2020; Zhou *et al*., 2021, Manning *et al*., 2012), even when considering different tracers and methods, analyzed the water's MTT or mean residence time during a short period of time (1 to 2 years), which meant that there was still a need to understand the long-term changes after forest change.

To make sure that the methodology process is the best approach for this study, we compared the methodology being done without the SF_6 apparent age preliminary information. This random approach took longer to reach results because it only considered trial-and-error, and the RMSE was also higher on the end compared to the methodology with SF_6 apparent age. This shows that our methodology takes less times to reach the lowest error according to the EPM. Our methodology needs less trials during the parameter search, and is the one with the lowest error.

Additionally, even though previous studies have shown that rainfall and throughfall or stemflow can have different isotopic signals (Pinos *et al*., 2022), there are others that have effectively estimated the MTT of groundwater and stream water by measuring precipitation stable isotopes samples (Jung *et al*., 2020). In our study area, the use of precipitation isotopic information makes it possible to know the average values of rain that inputs there, which do not show large variation from the throughfall data, and because of that, we can focus on the relative change of MTT. Also, we have a longer dataset of precipitation that makes the estimation of MTT in the short and long-term possible.

Generally, an increase of 1% in evaporation of raindrops causes deuterium excess to decrease by approximately 1‰ (Wang, *et al*., 2016). The isotopic composition of precipitation

and river runoff in the vicinity of the North American Great Lakes was also characterized by increased deuterium-excess, suggesting mixing of recycled evaporated moisture from the lake surface (Ichiyanagi, 2007). According to those results, we can understand the difference of the d-excess values depending on the period of time in the precipitation at our study area. That being said, we found that Before Thinning and Long After Thinning, the water d-excess in general is lower, which shows the impact of evapotranspiration in this component. This indicates there is higher evapotranspiration during these two periods, including more evaporation caused by the interception of a higher number of trees (especially Before Thinning).

Thus, it is possible to confirm that in this study's small headwater catchment at a plantation forested mountain in Japan, the thinning treatment affected the hydrological processes for the first few years after the treatment. Soon After Thinning, the higher MTT indicates increase of groundwater level, storage volume, mixing and alteration of subsurface flow. Kikuchi (2022), has found results at the same study area that show when the groundwater level changes, the flow direction also is altered, which can explain the different MTTs found from the Soon After Thinning period to the Long After Thinning one.

According to the findings in Sakakibara *et al*., 2019, the SF_6 ages of springs undergo seasonal changes, which we also observed in this study. The SF_6 water age analyses in (Busenberg and Plummer 2000, Manning *et al*., 2012, Santoni *et al*., 2016, Hale *et al*., 2016) were similar to those conducted in this study, such as using a short sampling period to analyze and obtain SF_6 ages, mean ages obtained found from a mixed-age sample, and mean ages that were flow-weighted from the discharging water. In addition, large annual variations in the SF_6 age have been observed. Suzuki (2022) has found results at the same study area that show when the spring water discharge is low, the SF_6 apparent age has a large variation (very young or very old). But when the spring water discharge is high, SF_6 apparent age is younger in a more stable way.

Differently from previous studies, we have applied this new methodology according to the SF_6 apparent age data as it is an indicative of the real water age of the samples. This way, the parameters search, model calibration and fitting process are not calculated exclusively by trial-and-error, as there is an initial parameter that can be found from previous data analysis and, therefore, it is an initial estimation based on theoretical knowledge. That is why we consider the SF_6 apparent age weighted average as an initial facilitator of the modelling process, but not as the final result itself.

The apparent age and MTT are a result of mixture of multiple flow paths with a different apparent age/MTT, so they tend to change temporally even during the time scale of rainstorm events. Besides, MTT was estimated using multiple groundwater flow paths that have different transit times and could change daily, seasonally and annually de-pending on the mixing ratio of the different groundwater flow paths. Considering that we wanted to understand the long-term temporal variations in MTT, there was a need to properly organize the data to observe any changes that occurred during the entire study period.

Therefore, we set our research question as to verify and understand the short and long-term temporal changes in MTT after the forest had a thinning treatment, thus we believe that the focus of the results should be on three periods: “before thinning” (June 2010–September 2011), “soon after thinning” (November 2011–December 2013), and “long after thinning” (August 2017–November 2021).

The annual water balance information supports the results of this study, which shows that an increasing MTT reflects the increased infiltration, groundwater levels, storage volume and the decreased water loss. Since we could estimate a decrease of MTT long after thinning, this indicates a change of volume storage declining six years after thinning, which is an opposite tendency from the previous study period.

Changes in vegetation cover could also have occurred in the catchment throughout the study

period. Such variations may be associated with an understory vegetation post-recovery phase, as forest thinning had occurred several years prior. Therefore, we suggest that future studies should include information on vegetation cover recovery in addition to hydrological data. Consequently, we stress that the effects of forest thinning on hydrological processes in small headwater catchments are extensive. The impacts caused by thinning were observed soon after thinning occurred because of the MTT, followed by increases in storage volume during the following two years. In contrast, six years after thinning, the impacts were smaller and hydrological processes returned to their original status trend, as demonstrated by the lower MTT and storage volume.

As it has been shown by previous research, after the reduction of forest cover, water yield increase was found in the first couple of years. Later, it diminished as the forest regrew. In this study, the impacts caused by thinning were observed soon after thinning occurred, because of the higher MTT, increases in storage volume during the next 2 years.

Intensive thinning in a small headwater plantation was effective to increase net precipitation and stream water for a short period. In this study, 6 years after thinning, the impacts were smaller and hydrological processes returned to their original status, as demonstrated by the lower MTT and storage volume values.

High-intensity (62%) thinning on Japanese cypress plantation forests increases (50–133%) in subsurface flow, with a link in increased baseflow runoff to reduced transpiration, according to Kuraji et al., 2019). There are few catchments with long and detailed tracer records to use many of the tracer techniques to document MTTs.

Although some studies have shown that regional water budgets may be positively affected by increasing forest and wetland cover (Ellison *et al*., 2012), we understand that this field of study depends on the area in which it is being investigated and its specific characteristics. As different hydrological responses to forest disturbances in distinct watersheds are also due to

their particular characteristics (Zhang *et al*., 2014).

The annual water balance information supports the results of this study, which are similar to other studies in small headwater forested catchments, which shows higher runoff and groundwater levels soon after thinning of forest (Chiu *et al*., 2022), and even global ones (Zhang *et al*., 2017; Li *et al*., 2017).

On Chiu et al., 2022, evapotranspiration decreased because of the removal of canopy trees. However, there is a decrease in treatment effect in evapotranspiration 5 months after thinning. This may be partially explained by the interception and transpiration from the regrowth understory vegetation. Evapotranspiration decreased because of the removal of canopy trees. However, there is a decrease in treatment effect in evapotranspiration 5 months after thinning. This may be partially explained by the interception and transpiration from the regrowth understory vegetation. These findings can be compared to this study because they were done in the same area during the thinning activities period. Their post-thinning trend shows higher runoff and GWL compared to Pre-thinning. These findings are similar to our and when we analyze the high rainfall event for each study period, the trend that the long after thinning period has lower effects from thinning treatments can be confirmed (Figure 30).

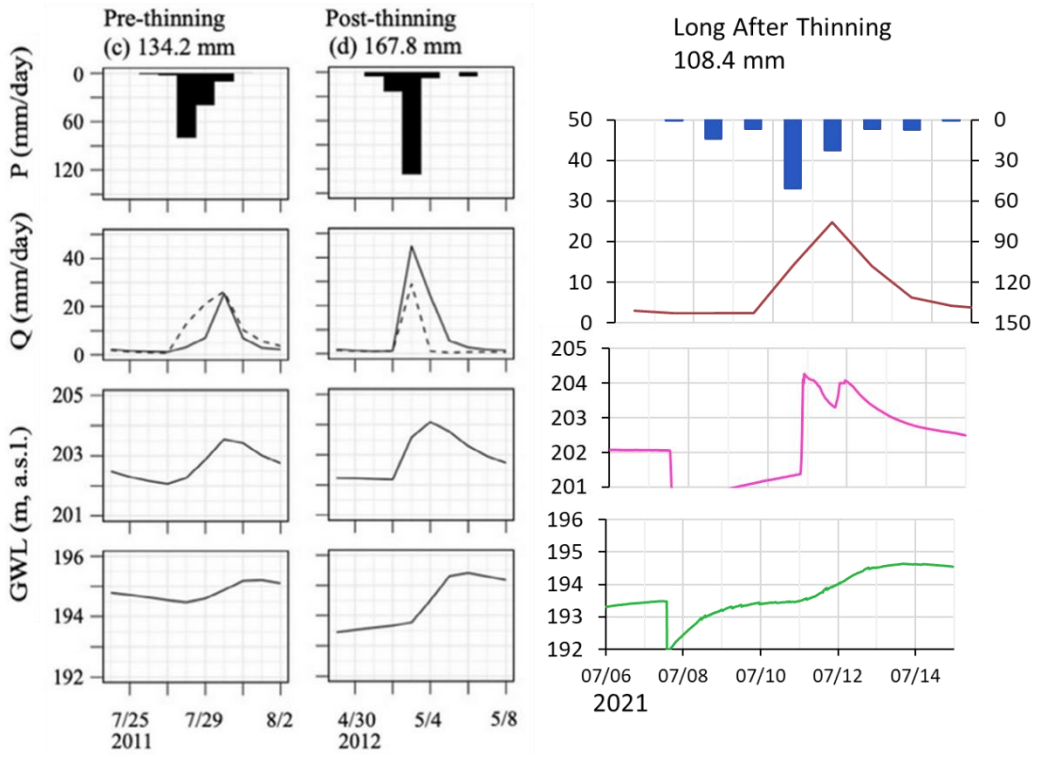

Figure 30. Comparison of high rainfall events from Chiu *et al*., 2022 and this study.

CHAPTER 6 CONCEPTUAL MODEL

According to the results and discussion, we can see that the volume at the KS2-5 catchment has an increase Soon After Thinning of the forest, and then, from 4 to 8 years Long After Thinning, it starts to decrease again. In addition, it should be noted that there is a vegetation cover change at the KS2-5 catchment throughout the years. The same location shows a vegetation change from 2013, during the Soon After Thinning period, to 2021, the Long After Thinning period. This variation can be associated with a post-recovery phase of the understory vegetation, since the thinning was applied a few years ago already, which means a potential increase of evapotranspiration at the area. Therefore, the Soon After Thinning period has lower evapotranspiration than the Before Thinning and Long After Thinning periods.

In addition, we can see in the observed data that the groundwater level increased to 202.6 (GW 15m) and 194.2 (GW 30m) in the Soon After Thinning period. Then, in the Long After Thinning period, the groundwater level decreased to 201.5 (GW 15m) and 191.4 (GW 30m). These similar changes and patterns were also observed in the runoff data at the study area. Because of these evidences, we can understand that higher infiltration rates in the Soon After Thinning period have occurred. This infiltration caused a higher mixing with older groundwater (deeper groundwater mixing), which is reflected in the increase of MTT and makes older water discharge at the spring point.

In contrast, lower infiltration rates in the Long After Thinning period have occurred (which show some similarity to the Before Thinning period). This caused a mixing with older water that is not as high as the Soon After Thinning period, and not as low as the Before Thinning period. This is reflected in the decrease of MTT and makes younger water discharge at the spring point.

Taking all these into consideration, we can see that the long-term variation of MTT show

that forest thinning affects the hydrological processes, and the subsurface changes last longer than the surface ones. Therefore, the longer values of MTT indicate an increase of groundwater volume storage, and shorter values of MTT indicate a decrease of groundwater volume storage. This is further shown in the schematic of the conceptual model of the study area (Figure 31).

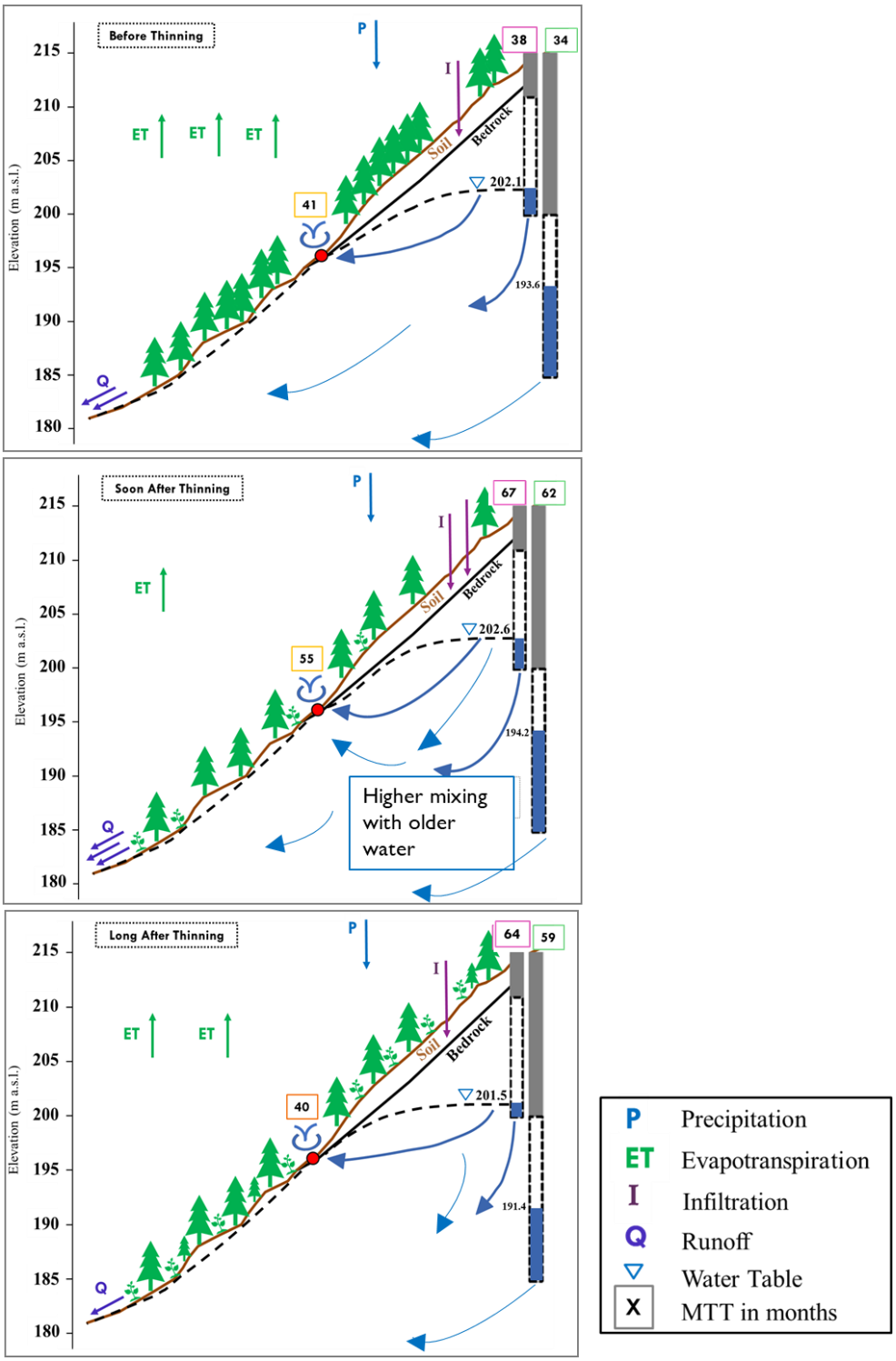

Figure 31. Schematic diagram illustrating the hydrological processes in the study area during the observation period. The number of arrows demonstrate the changes in the amount of ET, Q and I, with the P arrow remaining stable. The water table line indicates fluctuations in groundwater storage volume.

CHAPTER 7 CONCLUSIONS

The purpose of this study was to determine how the characteristics of a forest alter the MTT and short and long-term hydrological processes in a forested headwater catchment. Previous studies have mainly investigated changes in hydrological processes soon after forest thinning was performed. We used a combination of water stable isotopes and SF_6 concentrations in the air and water to investigate temporal variations in the spring water and groundwater MTT and the effects of forest thinning on short and long-term hydrological processes.

One of the original aspects of this study is the application of a multi-tracer analysis to improve parameter search of MTT, which allowed the investigation of long-term temporal variations in the water MTT, making it possible to find the effects of forest thinning on short and long-term hydrological processes.

Therefore, a multi-tracer (SF_6 and stable isotopes) approach can find the MTT in a forested catchment after thinning and it is possible to know the change of hydrological processes on the long-term after the thinning treatment.

In addition, other original aspects of this study are:

- The establishment of what is the MTT change and its effect in the hydrological processes in a small forested headwater catchment after thinning
- Finding that the first 2 years after thinning have higher runoff and mixing with older groundwater, which is reflected in the increase of groundwater level and volume storage
- Finding that after 4 to 8 years of the thinning, the runoff and mixing with older groundwater are lower, which is reflected in the decrease of groundwater level and volume storage
- Show that the MTT reflect the increase of subsurface hydrological changes to forest thinning in the short-term and their return to the original condition in the long-term, which is a more gradual return than the surface change

This study demonstrates that a multi-tracer approach can assess and enhance the results of short and long-term variations in MTT and major hydrological processes. Moreover, we found that the characteristics of the hydrological processes underwent extended periods of changes following forest thinning. This knowledge is fundamental, as this topic has not been studied sufficiently. Investigations of hydrological responses to forest treatments demonstrate how the MTT and groundwater storage volume are quantitatively altered, which is essential for managing subsurface water resources in forested regions.

ACKNOWLEDGMENTS

I would like to express my gratitude to my supervisor Professor Dr. Maki Tsujimura, Faculty of Life and Environmental Sciences, University of Tsukuba, who has always supported me during my years in Tsukuba, since when I came as a Research Student, all through my Master Program and Doctoral Program years, guiding me to become a better researcher. It has been a long journey.

I would like to thank the Ministry of Education, Culture, Sports, Science, and Technology (MEXT) of Japan for their scholarship support during the doctoral program of this PhD candidate. I am grateful for the infrastructure at Mount Karasawa Experimental Forest, Tokyo University of Agriculture and Technology, and the facilities at the Hydrology and Water Environment Laboratory, Faculty of Life and Environmental Sciences of the University of Tsukuba, Japan.

My sincere thanks to all the members from the laboratory, who have always helped me during my sample collection and analysis during these years, in special Mr. Kashiwa and Mr. Imaizumi, Ms. Suzuki, Mr. Kikuchi and Ms. Kawabata, who were my partners during our field survey trips to Mount Karasawa. They were vital to allow me to endure the many field works we performed for a long time. I will always be grateful to our Team Karasawa.

Finally, I want to thank my friend and family, from Brazil, Japan and other countries as well, for their continuous support, kindness, understanding and help during these last six years. A special thanks goes to my fiancé, Yuri Lavinas, who showed me kindness, respect and love during these rough years of study that we both have been through. His unconditional support allowed me to persevere and thankfully we could both follow this post graduate journey together.

References

Asai, K., Tsujimura, M. and Satake, H. 2001. 乗鞍岳東斜面における地下水流動系と降雨流出過程. 日本水文科学会誌, 31, (4), 135-149. (in Japanese)

Asai K and Tsujimura M. 2010. 日本の都市域周辺における大気 SF_6 濃度の分布. 地下水学会誌, 59, (4), 345-354. (in Japanese)

Asai, K., Tsujimura, M., Fantong, W. Y., & Satake, H. 2011. Impact of natural and local anthropogenic SF_6 sources on dating springs and groundwater using SF_6 in central Japan. Hydrological Research Letters, 5, 42-46.

Asano Y, Uchida T, Ohte N. 2002. Residence time and flow paths of water in steep unchanneled catchments, Tanakami, Japan. *Journal of Hydrology*, **261**: 173-192. DOI: 10.1016/S0022-1694(02)00005-7

Asano, Y., H. Shibano, N. Tanaka, A. Ohkawa, & K. Asai. 2011. フロン類をトレーサに用いた西達布川源流湧水の平均滞留時間推定. 演習林, (50), 41-48. (in Japanese)

Busenberg E, Plummer LN. 2000. Dating young groundwater with sulfur hexafluoride: Natural and anthropogenic sources of sulfur hexafluoride. *Water Resources Research*, **36**: 3011-3030. DOI: 10.1029/2000WR900151

Busenberg, E., & Plummer, L. N. 2014. A 17-year record of environmental tracers in spring discharge, shenandoah national park, virginia, USA: Use of climatic data and environmental conditions to interpret discharge, dissolved solutes, and tracer concentrations. Aquatic Geochemistry, 20(2), 267-290.

Chiu, C.W.; Gomi, T.; Hiraoka, M.; Shiraki, K.; Onda, Y.; Dung, B.X. 2002. Evaluating changes in catchment-scale evapotranspiration after 50% strip-thinning in a headwater catchment. Hydrol. Process. 36, e14611. DOI: 10.1002/hyp.14611

Coplen, T. B. 1994. Reporting of stable hydrogen, carbon, and oxygen isotopic abundances

(Technical Report). Pure & Appl. Chem. 66, 273-276. DOI: /10.1351/pac199466020273

Craig, H. 1961. Isotopic Variations in Meteoric Waters. Science, 133, 1702-1703. http://dx.doi.org/10.1126/science.133.3465.1702

Dung BX, Hiraoka M, Gomi T, Onda Y, Kato H. 2015. Peak flow responses to strip thinning in a nested, forested headwater catchment. *Hydrological Processes*, **29**: 5098-5108. DOI: 10.1002/hyp.10720

Ellison, D.; Futter, M. N.; Bishop, K. On the forest cover-water yield debate: from demand-to supply-side thinking. Global Change Biology. 2012, 18, 806-820. DOI: 10.1111/j.1365-2486.2011.02589.x

Gleeson, T., Wada, Y., Bierkens, M.F. and van Beek, L.P., 2012. Water balance of global aquifers revealed by groundwater footprint. Nature, 488(7410), p.197.

Gooddy, D. C., Darling, W. G., Abesser, C., & Lapworth, D. J. 2006. Using chlorofluorocarbons (CFCs) and sulphur hexafluoride (SF_6) to characterise groundwater movement and residence time in a lowland chalk catchment. Journal of Hydrology, 330(1-2), 44-52.

Hale VJ, McDonnell JJ, Stewart MK, Solomon DK, Doolittle J, Ice GG, Pack RT. 2016. Effect of bedrock permeability on stream base flow mean transit time scaling relationships: 2. Process study of storage and release. *Water Resources Research*, **52**: 1375-1397. DOI: 10.1002/2015WR017660

Herrmann A, Finke B, Schoniger M, Maloszewski P and Sitcbdler W. 1990. The environmental tracer approach as a tool for hydrological evaluation and regionalization of catchment systems. *Regionalization in Hydrology*, **191**: 45-58.

Hotta, N., Tanaka, N., Sawano, S., Kuraji, K., Shiraki, K. and Suzuki, M., 2010. Changes in groundwater level dynamics after low-impact forest harvesting in steep, small watersheds. Journal of hydrology, 385(1-4), pp.120-131.

IAEA, 2006. Guidebook on the use of chlorofluorocarbons in hydrology. *Technical Report Series*,

438, 277p.

Ichiyanagi K. Review: Studies and Applications of Stable Isotopes in Precipitation. 2007. J. Jpn. Assoc. Hydrol. Sci., Vol. 37, No. 4, p. 165-185, 2007. Institute of Observational Research for Global Change (IORGC), Japan Agency for Marine-Earth Sciences and Technology (JAMSTEC)

Iwamoto, J., 2002. The development of Japanese forestry. Forestry and the forest industry in Japan, pp.3-9.

Jung YY, Koh DC, Lee J, Tsujimura M, Yun ST and Lee KS. 2020. Mean transit time and subsurface flow paths in a humid temperate headwater catchment with granitic bedrock. *Journal of Hydrology*, **587**: 124942 DOI: 10.1016/j.jhydrol.2020.124942

Kabeya N, Katsuyama M, Kawasaki M, Ohte N and Sugimoto A. 2007. Estimation of mean residence times of subsurface waters using seasonal variation in deuterium excess in a small headwater catchment in Japan. *Hydrological Processes*, **21**: 308-322. DOI: 10.1002/hyp.6231

Kamtchueng BT, Fantong WY, Wirmvem MJ, Tiodjio RE, Fouépé Takounjou A, Asai K, Bopda Djomou SL, Kusakabe M, Ohba T, Tanyileke G, Hell JV and Ueda A. 2015. A multi-tracer approach for assessing the origin, apparent age and recharge mechanism of shallow groundwater in the Lake Nyos catchment, Northwest, Cameroon. *Journal of Hydrology*, **523**: 790-803. DOI: 10.1016/j.jhydrol.2015.02.008

Kashiwa K, 2019. 堆積岩からなる山地源流域における湧水の滞留時間季節変動. Master's thesis, Graduate School of Life and Environmental Sciences, University of Tsukuba, 107p. (in Japanese)

Kawaguchi, S. 2013. Subsurface flow processes through soil and bedrock considering effect of thinning in a small headwater catchment underlain by sandstone. Master's thesis, Graduate School of Environmental Studies, University of Tsukuba, 151p.

Kikuchi K. 2022. 山地源流域における湧水の水文特性と微生物動態の関係. Master's thesis,

Graduate School of Environmental Studies, University of Tsukuba, 83p. (in Japanese)

Klaus, J. and McDonnell, J.J. 2013. Hydrograph separation using stable isotopes: Review and evaluation. Journal of Hydrology, 505, pp.47-64.

Komatsu, H., Kume, T. and Otsuki, K. 2010. Water resource management in Japan: Forest management or dam reservoirs? Journal of Environmental Management, 91(4), pp.814-823.

Komatsu, H., Tanaka, N. and Kume, T. 2007. Do coniferous forests evaporate more water than broad-leaved forests in Japan? Journal of Hydrology, 336(3-4), pp.361-375.

Kuraji K, Gomyo M and Nainar A. 2019. Thinning of cypress forest increases subsurface runoff but reduces peak storm-runoff: A lysimeter observation. *Hydrological Research Letters*, **13**: 49-54. DOI: 10.3178/hrl.13.49

Lane, P. N. J. and Mackay, S.M. 2001. Streamflow response of mixed-species eucalypt forests to patch cutting and thinning treatments. For. Ecol. Manag., 143, 131-142.

Lazo, P.X., Mosquera, G.M., McDonnell, J.J. and Crespo, P. 2019. The role of vegetation, soils, and precipitation on water storage and hydrological services in Andean Páramo catchments. Journal of Hydrology, 572, pp.805-819.

Li, Q.; Wei, X.; Zhang, M.; Liu, W.; Fan, H.; Zhou, G.; Giles-Hansen, K.; Liu, S.; Wang, Y. 2017. Forest cover change and water yield in large forested watersheds: A global synthetic assessment. Ecohydrology. 10, e1838. [DOI: 10.1002/eco.1838]

Lu, C.; Zhao, C.; Liu, J.; Li, K.; Wang, B.; Chen, M. Increased salinity and groundwater levels lead to degradation of the Robinia pseudoacacia forest in the Yellow River Delta. J. For. Res. 2022, 33, 1233-1245. DOI: /10.1007/s11676-021-01422-9

Małoszewski P and Zuber A. 1982. Determining the turnover time of groundwater systems with the aid of environmental tracers: 1. Models and their applicability. *Journal of Hydrology*, **57**: 207-231

Manning AH, Clark JF, Diaz SH, Rademacher LK, Earman S, Plummer LN. 2012 Evolution of

groundwater age in a mountain watershed over a period of thirteen years. *Journal of Hydrology*, **460-461**: 13-28. DOI: 10.1016/j.jhydrol.2012.06.030

Marui, A. 1991. Rainfall-runoff process and function of subsurface water storage in a layered hillslope. Geographical Review of Japan 64: 145-166. (JE)

McGuire, K.J., DeWalle, D.R. and Gburek, W.J., 2002. Evaluation of mean residence time in subsurface waters using oxygen-18 fluctuations during drought conditions in the mid-Appalachians. Journal of Hydrology, 261(1-4), pp.132-149.

McGuire KJ and McDonnell JJ. 2006. A review and evaluation of catchment transit time modeling. *Journal of Hydrology*, **330**: 543-563. DOI: 10.1016/j.jhydrol.2006.04.020

McNamara, J.P., Tetzlaff, D., Bishop, K., Soulsby, C., Seyfried, M., Peters, N.E., Aulenbach, B.T. and Hooper, R., 2011. Storage as a metric of catchment comparison. Hydrological Processes, 25(21), pp.3364-3371.

Momiyama H, Kumagai T and Egusa T. 2021. Model analysis of forest thinning impacts on the water resources during hydrological drought periods. *Forest Ecology and Management*, **499**: 119593. DOI: 10.1016/j.foreco.2021.119593

Muñoz-Villers LE, McDonnell JJ. 2012. Runoff generation in a steep, tropical montane cloud forest catchment on permeable volcanic substrate. Water Resour. Res., 48 (9), Article W09528, DOI: 10.1029/2011WR011316

Nam, S.; Hiraoka, M; Gomi, T.; Dung, B. X.; Onda, Y.; Kato, H. 2016. Suspended-sediment responses after strip thinning in headwater catchments. Landscape Ecol Eng. 12, 197-208. DOI: 0.1007/s11355-015-0284-0

Newton, B.T., Mamer, E., ReVelle, P. and Garduño, H. 2015. Sacramento Mountains Watershed Study–The Effects of Tree Thinning on the Local Hydrologic System. New Mexico Bureau of Geology and Mineral Resources Open-File Report.

Onda Y, Gomi T, Mizugaki S, Nonoda T and Sidle RC. 2010. An overview of the field and

modelling studies on the effects of forest devastation on flooding and environmental issues. Hydrological Processes, 24: 527-534. DOI: 10. 1002/hyp. 7548

Pereira, L. C.; Balbinot, L.; Lima, M. T.; Bramorski, J.; Tonello, K. C. 2022. Aspects of forest restoration and hydrology: the hydrological function of litter. J. For. Res. 2022, 33, 543-552. DOI: 10.1007/s11676-021-01365-1

Pinos, J.; Llorens, P.; Latron, J. 2022. High-resolution temporal dynamics of intra-storm isotopic composition of stemflow and throughfall in a Mediterranean Scots pine forest. Hydrol. Process. 2022, 36, 8e14641. DOI: 10.1002/hyp.14641

Sakakibara, K., Tsujimura, M., and Asai K. 2017. Issues and prospects in estimating residence time of groundwater using sulfur hexafluoride (SF_6). 六フッ化硫黄 (SF_6) を用いた地下水の滞留時間推定における課題と展望 (in Japanese). Journal of the Japan Society of Groundwater Science, 59 (2), pp.87-103.

Sakakibara K. 2018. Age Dating of Rainfall-runoff Water with Sulfur Hexafluoride and Discharge Processes in a Forested Headwater Catchment. PhD thesis, Graduate School of Life and Environmental Sciences, University of Tsukuba, 159p

Sakakibara K, Tsujimura M, Iwagami S, Sato Y, Nagano K, Onda Y. 2019. Effectivity of dissolved SF_6 tracer for clarification of rainfall-runoff processes in a forested headwater catchment. Hydrological Processes, **33**: 892-904. DOI: 10.1002/hyp.13398

Santoni S, Huneau F, Garel E, Vergnaud-Ayraud V, Labasque T, Aquilina L, Jaunat J, Celle-Jeanton H. 2016. Residence time, mineralization processes and groundwater origin within a carbonate coastal aquifer with a thick unsaturated zone. *Journal of Hydrology*, **540**: 50-63. DOI: 10.1016/j.jhydrol.2016.06.001

Soulsby C, Tetzlaff D and Hrachowitz M. 2009. Tracers and transit times: Windows for viewing catchment scale storage? *Hydrological Processes*, **23**: 3503-3507, DOI:10.1002/hyp.7501

Sprenger M, Stumpp C, Weiler M, Aeschbach W, Allen ST, Benettin P, Dubbert M, Hartmann A,

Hrachowitz M, Kirchner JW, McDonnell JJ, Orlowski N, Penna D, Pfahl S, Reinderer M, Rodriguez N, Schmidt M, Werner C. 2019. The demographics of water: A review of water ages in the critical zone. *Reviews of Geophysics*, **57**. DOI:10.1029/ 2018RG000633

Stadler S, Osenbrück K, Suckow AO, Himmelsbach T and Hötzl H. 2010. Groundwater flow regime, recharge and regional-scale solute transport in the semi-arid Kalahari of Botswana derived from isotope hydrology and hydrochemistry. *Journal of Hydrology*, **388**: 291-303. DOI: 10.1016/j.jhydrol.2010.05.008

Stewart M K, Morgenstern U, Tsujimura M, Gusyev M A, Sakakibara K, Imaizumi Y, Rutter H, van der Raaij R, Etheridge Z, Scott L, Cox S C. 2018. Mean residence times and sources of Christchurch springs. *Journal of Hydrology (New Zealand)*, **57**: 81–94. https://www.jstor.org/stable/26643851

Sun X, Onda Y, Kato H, Gomi T and Komatsu H. 2015. Effect of strip thinning on rainfall interception in a Japanese cypress plantation. *Journal of Hydrology*, **525**: 607-618. DOI: 10.1016/j.jhydrol.2015.04.023

Suzuki A. 2022. 堆積岩からなる山地源流域における湧水の滞留時間変動. Master's thesis, Graduate School of Environmental Studies, University of Tsukuba, 105p. (in Japanese)

UNITED NATIONS, 2019. Sustainable Development Goals, Goal 6: Clean Water and Sanitation. Accessed on December 15, 2022: https://www.un.org/sustainabledevelopment/water-and-sanitation/.

Vachier, P., Dever, L. and Fontes, J.C., 1987. Water movements in the unsaturated zone and supply of the Champagne Chalk Nappe (France): isotopic and chemical approaches (in French) Mouvements de l'eau dans la zone non saturee et alimentation de la Nappe de la Craie de Champagne (France): approches isotopique et chimique. In International symposium on the use of isotope techniques in water resources development (pp. 367-379).

Wang, S., Zhang, M., Che, Y., Zhu, X., & Liu, X. 2016. Influence of Below-Cloud Evaporation on

Deuterium Excess in Precipitation of Arid Central Asia and Its Meteorological Controls, *Journal of Hydrometeorology*, *17*(7), 1973-1984.

Yaginuma T. 2015. 山地源流域の人工林における間伐前後の水文プロセス変動. Master's thesis, Graduate School of Environmental Studies, University of Tsukuba, 151p. (in Japanese)

Yasuhara, M., Kazehaya, K. and Marui, A. 2007. 富士山の地下水とその涵養プロセスについて. 荒牧重雄・藤井敏嗣・中田節也・宮地直道編「富士火山」山梨県環境科学研究所, 389-405. (in Japanese)

Zhang, M.; Wei, X. 2014. Contrasted hydrological responses to forest harvesting in two large neighbouring watersheds in snow hydrology dominant environment: implications for forest management and future forest hydrology studies. Hydrol. Process. 28, 6183-6195. [DOI: 10.1002/hyp.10107]

Zhang, M.; Liu, N.; Harper, R.; Li, Q.; Liu, K.; Wei, X. Ning, D. Hou, Y.; Liu, S. 2017. A global review on hydrological responses to forest change across multiple spatial scales: Importance of scale, climate, forest type and hydrological regime. J. Hydrol 546, 44-59. [DOI: 10.1016/j.jhydrol.2016.12.040]

Zhou J, Liu G, Meng Y, Xia CC, Chen K and Chen Y. 2021. Using stable isotopes as tracer to investigate hydrological condition and estimate water residence time in a plain region, Chengdu, China. *Scientific Reports*, **11**: 2812. DOI: 10.1038/s41598-021-82349-3

ANNEX

A1. Hydrological Data

Date	Spring Water					GW 15m					GW 30m				
	pH	EC (μS/cm)	ORP (mV)	DO (mg/L)	Temp (°C)	pH	EC (μS/cm)	ORP (mV)	DO (mg/L)	Temp (°C)	pH	EC (μS/cm)	ORP (mV)	DO (mg/L)	Temp (°C)
2017/5/23	6.82	78.0	306	8.80	13.0										
2017/9/14	7.46	103.0	133	8.56	14.3	6.22	83.0	277	6.96	14.2	6.52	69.0	256	6.96	14.5
2017/10/13	7.16	128.0	242	7.00	14.4	7.12	111.1	274	6.60	13.9	6.75	109.0	184	5.00	13.9
2017/11/10	7.23	110.0	233	9.50	13.9	6.45	97.0	249	6.30	13.9	6.94	92.0	69	5.80	14.0
2017/12/8	7.30	62.2	210	9.60	13.2	6.35	102.0	342	11.50	13.3	6.59	96.8	311	9.70	13.3
2018/3/22	7.69	128.0	144	2.53	12.1	6.42	152.0	240	3.58	13.3	6.53	142.0	71	2.76	13.4
2018/4/25	7.37	119.0	211	4.11	12.9	6.46	134.0	260	3.13	15.1	6.73	146.0	248	2.38	14.1
2018/6/27	7.85	86.0	134	4.08	14.0	6.96	97.0	110	4.03	15.1	7.24	118.0	92	2.04	14.8
2018/7/20	7.88	92.0	126	7.70	15.0	6.55	86.0	237	5.42	15.8	6.85	73.5	135	2.64	15.6
2018/8/27	7.42	84.0	98	8.40	14.9	6.27	1.4	261	5.07	14.8	6.73	124.0	127	4.20	15.0
2018/9/12	7.15	90.0	118	8.20	14.7	6.48	127.0	273	6.24	14.6	6.98	103.0	99	6.38	14.8
2018/9/25	6.92	121.0	107	6.70	14.7	6.87	96.0	167	5.77	14.2	7.02	126.0	106	5.48	13.8
2018/11/2	6.70	108.0	132	7.47	13.9	6.70	86.0	205	4.60	13.8	6.20	73.0	114	5.73	13.4
2018/11/22	6.72	98.0	149	7.23	13.5	6.25	98.0	188	5.76	13.6	6.40	78.0	124	4.90	13.4
2019/4/24						6.30	80.0	125	8.50	14.3	6.30	73.0	194	5.13	13.8
2019/6/5	6.00	85.5	205	8.30	13.6	5.80	64.3	209	7.85	15.7	5.70	66.3	232	5.79	14.5
2019/8/7	6.70	89.0	114		17.4	6.00	69.0	117		15.1	6.50	65.0	121		14.5
2020/8/11	7.50	82.0		6.99	14.7	7.40	121.0	307	7.65	16.0	7.60	77.0	136	8.56	15.8
2020/11/26	6.24		92		11.4										
2021/1/27	7.50	92.0	273	10.58	8.4	7.00	76.0	268	10.55	13.6	7.20	75.0	232	6.07	13.7
2021/2/17	6.60	92.0	293	11.64	6.4	6.10	81.0	92	11.07	12.4	6.80	85.0	97	7.84	13.2
2021/3/31	7.60	79.0	38	11.06	12.5		75.0	66	9.35	14.4					
2021/4/14	7.50	81.0	266	9.16	12.5	7.20	75.0	74	9.17	14.5	7.10	73.0	126	6.34	14.3
2021/4/28	7.40	90.0	240	9.79	12.7	6.70	86.0	74	8.52	14.3	6.80	85.0	73	7.66	14.0
2021/5/12	6.50	70.0	274	8.23	13.4	5.40	63.0	135	8.63	14.8	6.10	64.0	122	6.13	14.2
2021/5/26	6.92	78.0	276	6.19	13.2	6.22	66.0	109	5.29	14.5	6.35	75.0	107	5.67	14.1
2021/6/9	6.30	68.0	297	5.47	13.4	6.01	79.0	115	5.55	14.5	6.40	70.0	112	4.39	15.4
2021/6/23	6.30	55.0	68	7.17	13.3	6.10	64.0	101	5.61	14.7	6.30	78.0	65	5.37	14.5
2021/7/7	7.00	61.0	83	7.52	13.3	6.50	71.0	83	5.54	15.5	6.70	71.0	89	6.31	15.2
2021/7/21	6.80	64.0	73	7.37	13.8	6.40	69.0	77	5.85	14.7	6.70	69.0	83	4.65	14.8
2021/8/4	7.00	66.0	90	6.07	14.2	6.80	81.0	88	6.12	14.2	6.00	67.0	91	5.38	14.4
2021/8/19	6.80	72.0	60	6.05	14.1	6.50	73.0	84	6.79	15.5	6.70	77.0	107	5.42	14.7
2021/9/28	7.20	78.0	108	7.13	14.4	6.50	77.0	121	6.88	13.8	6.40	73.0	72	9.95	14.0
2021/10/13	6.00	71.0	255	10.92	14.3	6.10	73.0	280	7.59	13.9	6.20	74.0	292	6.00	13.8
2021/10/28	6.40	82.0	268	11.64	14.0	6.10	79.0	111	9.59	13.7	6.60	71.0	114	9.63	13.7
2021/11/10	6.58	77.0	241	9.23	14.0	6.60	78.0	217	6.78	13.6	6.00	74.0	182	6.30	13.6
2021/11/24	6.60	81.0	245	6.96	13.7	6.50	76.0	158	7.98	13.4	6.70	71.0	232	6.80	13.3

A2. Stable Isotopes data

	Spring Water				GW 15m				GW 30m			
Date	δ 18O ‰	δ 2H ‰	d-excess	Runoff mm/d	δ 18O ‰	δ 2H ‰	d-excess	GWL masl	δ 18O ‰	δ 2H ‰	d-excess	GWL masl
2010/7/7	-8.65	-55.50	13.71		-8.66	-55.43	13.85	202.5	-8.53	-56.56	11.68	193.8
2010/7/15	-8.59	-55.59	13.11		-8.51	-55.50	12.56	202.6	-8.50	-55.81	12.22	194.1
2010/7/24	-8.48	-55.95	11.86		-8.53	-54.66	13.57	202.0	-8.56	-54.81	13.70	193.8
2010/9/17					-8.53	-55.28	12.96		-8.44	-55.90	11.64	192.4
2010/9/29	-8.44	-56.06	11.46		-8.31	-55.26	11.20		-8.35	-55.86	10.92	192.9
2010/11/5					-8.43	-55.35	12.05	202.5	-8.43	-55.95	11.47	194.0
2010/11/24	-8.44	-56.36	11.14		-8.33	-55.44	11.22	201.9	-8.41	-56.33	10.91	193.4
2010/12/2					-8.30	-55.21	11.21	201.8	-8.35	-55.59	11.17	193.3
2011/2/25	-8.52	-56.49	11.14									
2011/4/1								201.8				192.4
2011/5/28	-8.59	-56.50	12.24		-8.42	-55.58	11.81	201.7	-8.45	-55.61	12.02	192.3
2011/5/30					-8.52	-55.32	12.84	202.0	-8.53	-56.18	12.06	192.6
2011/5/31	-8.65	-56.53	12.64		-8.39	-55.38	11.73	201.8	-8.53	-56.25	11.99	192.6
2011/6/2					-8.44	-55.50	11.99	201.8	-8.55	-56.46	11.95	192.8
2011/6/6					-8.42	-55.62	11.73	201.8	-8.56	-56.50	12.00	193.1
2011/6/10					-8.50	-55.93	12.09	201.8	-8.59	-56.11	12.61	193.0
2011/7/18	-8.38	-56.16	10.90	0.4544	-8.37	-55.71	11.29	201.8	-8.47	-56.23	11.55	192.9
2011/7/20	-8.54	-56.24	12.06	1.2440	-8.35	-55.51	11.33	204.1	-8.41	-56.47	10.80	193.4
2011/7/21					-8.22	-55.04	10.70	203.7	-8.38	-55.99	11.02	194.5
2011/8/3	-8.58	-57.08	11.54	1.7409	-8.29	-54.60	11.71	202.6	-8.28	-55.19	11.06	195.0
2011/9/20					-8.04	-56.26	8.09	201.9	-8.14	-56.59	8.50	194.4
2011/9/21				2.3455	-8.12	-56.16	8.82	201.9	-8.11	-56.67	8.21	194.4
2011/9/23					-8.14	-56.00	9.09	203.8	-8.14	-56.57	8.54	195.2
2011/10/3	-8.15	-56.84	8.39	0.2755	-8.21	-56.00	9.70	202.1	-8.14	-56.42	8.70	194.7
2011/12/2				0.0768	-8.21	-52.31	13.39	201.9	-8.20	-52.45	13.16	193.5
2012/1/9	-8.29	-52.80	13.49	0.1449	-8.02	-52.19	12.00	201.8	-8.18	-52.83	12.65	192.4
2012/2/19	-8.28	-52.98	13.25	0.0785	-7.97	-51.89	11.90	201.8	-8.17	-52.77	12.56	191.9
2012/4/6	-8.15	-53.05	12.16	0.3762	-8.13	-52.05	12.99	202.0	-7.94	-52.08	11.43	193.6
2012/5/13	-8.29	-52.08	14.21	0.0003	-8.19	-51.48	14.04	202.5	-8.20	-52.28	13.33	195.0
2012/5/31	-8.15	-52.59	12.63	0.0003	-8.16	-52.08	13.21	202.3	-8.26	-52.54	13.52	194.4
2012/6/19	-8.11	-52.65	12.23	0.1453	-8.15	-52.61	12.55	202.0	-8.16	-53.03	12.28	194.4
2012/6/27	-8.29	-52.87	13.48	0.1476	-8.16	-51.82	13.44	202.3	-8.24	-52.63	13.26	195.0
2012/7/5	-8.22	-53.59	12.15	0.1148	-8.13	-52.33	12.68	202.2	-8.27	-52.61	13.53	194.7
2012/8/11	-8.30	-54.12	12.28		-8.14	-52.32	12.77	202.0	-8.17	-52.79	12.54	194.2
2012/8/28	-8.02	-53.51	10.64		-7.96	-52.50	11.26	201.9	-8.00	-52.73	11.21	193.7
2012/9/30	-7.92	-52.22	11.16		-7.87	-52.07	11.69		-8.00	-52.33	10.87	
2012/11/3	-8.07	-52.26	12.30		-7.97	-52.49	11.56		-8.00	-52.46	11.27	
2013/7/2	-8.10	-52.81	11.97		-8.30	-52.73	13.67		-8.09	-51.92	12.76	
2013/7/26	-8.15	-51.88	13.30		-8.04	-52.42	11.92		-8.10	-53.23	11.53	
2013/7/31	-8.01	-51.35	12.69		-8.08	-51.67	12.97		-8.29	-52.44	13.84	
2013/9/1	-7.83	-51.02	11.66		-8.36	-54.24	12.65		-8.07	-52.44	12.10	
2013/9/15	-6.96	-45.85	9.87		-8.02	-51.88	12.29		-8.10	-51.96	12.83	
2013/9/18	-7.92	-50.54	12.82		-7.68	-50.14	11.27		-8.03	-52.20	12.04	

A3. SF_6 concentration data

	Spring Water			GW 30m		
Date	SF6 years	SF6 years (fmol/L)	SF6 (pptv)	SF6 years	SF6 years (fmol/L)	SF6 (pptv)
2017/5/23	2.6	4.0	11.8			
2017/9/14	1.1	4.28	12.68			
2017/10/13	10.3	2.97	8.79			
2017/11/10	7.0	3.43	10.15			
2017/12/8	0.2	4.46	13.20	2.8	4.0	11.96
2018/3/22	5.2	3.72	11.02	8.4	3.3	9.72
2018/4/25	10.9	2.96	8.76	10.0	3.1	9.15
2018/6/27	4.9	3.82	11.32	2.7	4.1	12.28
2018/7/20	1.7	4.33	12.82	1.9	4.3	12.72
2018/8/27	2.2	4.25	12.60	2.0	4.3	12.69
2018/9/12	3.1	4.12	12.19	2.0	4.3	12.70
2018/11/2	9.2	3.25	9.62	2.7	4.2	12.42
2018/11/22	5.4	3.78	11.21	2.5	4.2	12.58
2019/4/24	3.6	4.07	12.06			
2019/6/5						
2019/8/7						
2020/8/11						
2020/11/26	21.0	1.51	4.76			
2021/1/27				13.5	2.14	6.75
2021/2/17	17.0	1.83	5.79			
2021/3/31	10.5	2.44	7.69			
2021/4/14	5.5	2.91	9.21			
2021/4/28		4.88	15.42	12.5	2.23	7.05
2021/5/12	3.5	3.16	9.97			
2021/5/26	6.5	2.9	9.07			
2021/6/9	6.5	2.84	8.98			
2021/6/23	5.0	2.99	9.46	5.0	3.0	9.4
2021/7/7	1.5	3.4	10.72		4.2	13.3
2021/7/21		4.6	10.64		4.3	13.6
2021/8/4	3.0	3.3	9.44	2.5	3.3	10.5
2021/8/19			12.41	2.0	3.4	10.6
2021/9/28	5.5	2.97	9.38			
2021/10/13	2.5	3.36	10.62	2.5	3.3	10.6
2021/10/28	0.5	3.76	11.88	0.5	4.2	13.2
2021/11/10	0.5	3.70	11.68	0.5	4.2	13.1
2021/11/24	0.5	3.83	12.09	1.0	3.5	11.1

A4. R software Code

```
library(dplyr)
library("signs")
library("ggplot2")
setwd("C:¥¥/Users/ /OneDrive/ / /")
amplitudeEstimation <- function(A, k, filename) {
  ## reading data of observed output
  data = read.csv(filename)
    observed = data$Observed
      times = data$Tempo
    omega = (2 * pi / 12) # a whole year cycle
      mean_observed = mean(data$Observed[!is.na(data$Observed)])
    calculated = mean_observed + A * sin(omega * times +4) + k * times
  observed = data$Observed[!is.na(data$Observed)]
  din_calculated = calculated[!is.na(data$Observed)]
  n = length(observed)
    upper = sum((observed - din_calculated) ^ 2)
  rmse = sqrt(upper / n)
    out = list(rmse = rmse, calculated = calculated, observed = data$Observed, Time = data$Date)
    return(out)
  return(rmse)
}
EPM  <- function(beta,
                 tau,
                 A = init_A,
                 k = 0,
                 filename) {
  data = read.csv(filename)
  times = data$Tempo
    B = A / sqrt(1 + (omega ^ 2 * tau ^ 2) / (beta ^ 2))
    term1 = omega * tau * (1 - (1 / beta))
    inner = 1 / (sqrt (1 + ((omega ^ 2 * tau ^ 2) / beta ^ 2)))
  term2 = acos(inner)
    phi = term1 - term2
    calculated = mean(data$Observed[!is.na(data$Observed)]) + B * sin(omega * times + phi) + k
   *    (times - tau)
    observed = data$Observed
    observed = data$Observed[!is.na(data$Observed)] # without noise
  dout_calculated = calculated[!is.na(data$Observed)] # without noise
  n = length(observed)
    upper = sum((observed - dout_calculated) ^ 2)
  rmse = sqrt(upper / n)
  rmse = round(rmse, 3)
    out = list(rmse = rmse, calculated = calculated, observed = data$Observed, Time = data$Date)
    return(out)
```

```
} #13.42
As = seq(0, 30 , by = 0.01)
taus = seq(1, 80, by = 0.1)
betas = seq(1, 2, by = 0.01)
print("Complete year interval 2010-21")
filename_all = ('PrecipitationDexcessAll2010-2021.csv')
out_all = sapply(
  As,
  amplitudeEstimation,
  filename = filename_all,
  k = 0
)
As_error = unlist(out_all[1,])
As_error = unlist(out_all[1,])
calculated_all = unlist(out_all[2,which.min(As_error)])
observed_all = unlist(out_all[3,1])
times_all = unlist(out_all[4,1])
A_found = As[which.min(As_error)]
out_out1 = sapply(betas,
                  EPM,
                  tau = 39.1,
                  A = A_found,
                  filename = filename_out)
beta_errors = unlist(out_out1[1,])
out_out = sapply(taus,
                 EPM,
                 A = A_found,
                 beta = betas[which.min(beta_errors)],
                 filename = filename_out)
taus_errors = unlist(out_out[1,])
calculated_out = unlist(out_out[2,which.min(taus_errors)])
observed_out = unlist(out_out[3,1])
times_out = unlist(out_out[4,1])
taus[which.min(taus_errors)]
cat("When beta = ",
    betas[which.min(beta_errors)],
    ", tau =",
    taus[which.min(taus_errors)],
    ', with error =',
    taus_errors[which.min(taus_errors)],
    '¥n')
observed_data = rbind(cbind(observed_out, "observed_out", times_out),
                      cbind(observed_all[1:31], "observed_all",times_all[1:31]))
calculated_data = rbind(
  cbind(calculated_out, "calculated_out", times_out),
  cbind(calculated_all[1:31], "calculated_all",times_all[1:31]))
```

```
observed_data = as.data.frame(observed_data)
calculated_data = as.data.frame(calculated_data)
colnames(observed_data) = c("data", "name", "times")
colnames(calculated_data) = c("data", "name", "times")
observed_data$data = as.numeric(observed_data$data)
observed_data=observed_data[!is.na(observed_data$data),]

calculated_data$data = as.numeric(calculated_data$data)
calculated_data=calculated_data[!is.na(calculated_data$data),]
calculated_data$Date = as.Date(calculated_data$times, format = " %m/%d/%Y")
observed_data$Date = as.Date(observed_data$times, format = " %m/%d/%Y")
calculated_data=calculated_data[order(calculated_data$Date),]
observed_data=observed_data[order(observed_data$Date),]
calculated_data$times = factor(calculated_data$times, ordered = T)
calculated_data$times = factor(calculated_data$times, ordered = T)
before <- ggplot(data = observed_data,
                 aes(
                   x = Date,
                   y = data,
                   group = name,
                   fill = name
                 )) +
  geom_point(size = 4,
             stroke = 1.5,
             aes(color = name,
                 shape = name)) +
  geom_line(size = 1,
            data = calculated_data,
            aes(color = name,
                linetype = name)) +
  scale_shape_manual(values = c(1, 17), guide = "none") +
  scale_linetype_manual(values = c("solid", "twodash"), guide = "none") +
  scale_color_manual(values = c("#1F78B4", "#FF7F00", "#1F78B4", "#FF7F00"),
                     guide = "none") +
  scale_x_date(date_labels = "%Y/%m",
               date_breaks  = "3 month",
               name = "") +
  scale_y_continuous(breaks = round(seq(
    -1, 26, by = 5
  ), 2)) +
  ylab("d-excess (‰)") +
  theme_classic() +
  theme(axis.text.x = element_text(
    angle = 45,
    vjust = 1,
    hjust = 1
```

```
  ),
  axis.text = element_text(size = 16),
  axis.title = element_text(size = 18),
  legend.position = "none")
  plot(y = beta_errors, x = betas, ylab = "RSME", xlab = "Beta values", main = "RSME of the
   different Beta values in 2010-11")
plot(y = taus_errors, x = taus, ylab = "RSME", xlab = "Tau values", main = "RSME of the different
   Tau values in 2010-11")
observed_data_1_period = observed_data
calculated_data_1_period = calculated_data
print("YEAR 2011-13")
filename_in = (
  'PrecipitationDexcessInput-SoonAfterThinning2011-13.csv'
)
# set the filename that relates to the spring data
filename_out = ('SpringDexcessOutputSoonAfterThinning2011-13.csv')
out_out1 = sapply(betas,
                  EPM,
                  tau = 33.51,
                  A = A_found,
                  filename = filename_out)
beta_errors = unlist(out_out1[1,])
out_out = sapply(taus,
                 EPM,
                 A = A_found,
                 beta = betas[which.min(beta_errors)],
                 filename = filename_out)
taus_errors = unlist(out_out[1,])
calculated_out = unlist(out_out[2,which.min(taus_errors)])
observed_out = unlist(out_out[3,1])
times_out = unlist(out_out[4,1])
taus[which.min(taus_errors)]
cat("When beta = ",
    betas[which.min(beta_errors)],
    ", tau =",
    taus[which.min(taus_errors)],
    ', with error =',
    taus_errors[which.min(taus_errors)],
    '¥n')
observed_data = rbind(cbind(observed_out, "observed_out", times_out),
                      cbind(observed_all[35:83], "observed_all",times_all[35:83]))
calculated_data = rbind(
  cbind(calculated_out, "calculated_out", times_out),
  cbind(calculated_all[35:83], "calculated_all",times_all[35:83]))
observed_data = as.data.frame(observed_data)
calculated_data = as.data.frame(calculated_data)
```

```
colnames(observed_data) = c("data", "name", "times")
colnames(calculated_data) = c("data", "name", "times")
observed_data$data = as.numeric(observed_data$data)
observed_data=observed_data[!is.na(observed_data$data),]
calculated_data$data = as.numeric(calculated_data$data)
calculated_data=calculated_data[!is.na(calculated_data$data),]
calculated_data$Date = as.Date(calculated_data$times, format = " %m/%d/%Y")
observed_data$Date = as.Date(observed_data$times, format = " %m/%d/%Y")
calculated_data=calculated_data[order(calculated_data$Date),]
observed_data=observed_data[order(observed_data$Date),]
calculated_data$times = factor(calculated_data$times, ordered = T)
calculated_data$times = factor(calculated_data$times, ordered = T)
shortafter <- ggplot(data = observed_data,
                     aes(
                       x = Date,
                       y = data,
                       group = name,
                       fill = name
                     )) +
  geom_point(size = 4,
             stroke = 1.5,
             aes(color = name,
                 shape = name)) +
  geom_line(size = 1,
            data = calculated_data,
            aes(color = name,
                linetype = name)) +
  scale_shape_manual(values = c(1, 17), guide = "none") +
  scale_linetype_manual(values = c("solid", "twodash"), guide = "none") +
  scale_color_manual(values = c("#1F78B4", "#FF7F00", "#1F78B4", "#FF7F00"),
                     guide = "none") +
  scale_x_date(date_labels = "%Y/%m",
               date_breaks  = "3 month",
               name = "") +
  scale_y_continuous(breaks = round(seq(
    -1, 26, by = 5
  ), 2)) +
  ylab("d-excess (‰)") +
  theme_classic() +
  theme(axis.text.x = element_text(
    angle = 45,
    vjust = 1,
    hjust = 1
  ),
  axis.text = element_text(size = 16),
  axis.title = element_text(size = 18),
```

```
  legend.position = "none")
plot(y = beta_errors, x = betas, ylab = "RSME", xlab = "Beta values", main = "RSME of the
   different Beta values in 2011-13")
plot(y = taus_errors, x = taus, ylab = "RSME", xlab = "Tau values", main = "RSME of the different
   Tau values in 2011-13")
observed_data_2_period = observed_data
calculated_data_2_period = calculated_data
filename_in = (
  'PrecipitationDexcessInputLongAfterThinning2017-21.csv'
)
filename_out = ('SpringDexcessOutputLongAfterThinning2017-21.csv')
out_out1 = sapply(betas,
                  EPM,
                  tau = 39.11,
                  A = A_found,
                  filename = filename_out)
beta_errors = unlist(out_out1[1,])
out_out = sapply(taus,
                 EPM,
                 A = A_found,
                 beta = betas[which.min(beta_errors)],
                 filename = filename_out)
taus_errors = unlist(out_out[1,])
calculated_out = unlist(out_out[2,which.min(taus_errors)])
observed_out = unlist(out_out[3,1])
times_out = unlist(out_out[4,1])
taus[which.min(taus_errors)]
cat("When beta = ",
    betas[which.min(beta_errors)],
    ", tau =",
    taus[which.min(taus_errors)],
    ', with error =',
    taus_errors[which.min(taus_errors)],
    '¥n')
observed_data = rbind(cbind(observed_out, "observed_out", times_out),
                      cbind(observed_all[185:274], "observed_all",times_all[185:274]))
calculated_data = rbind(
  cbind(calculated_out, "calculated_out", times_out),
  cbind(calculated_all[185:274], "calculated_all",times_all[185:274]))
observed_data = as.data.frame(observed_data)
calculated_data = as.data.frame(calculated_data)
colnames(observed_data) = c("data", "name", "times")
colnames(calculated_data) = c("data", "name", "times")
observed_data$data = as.numeric(observed_data$data)
observed_data=observed_data[!is.na(observed_data$data),]
calculated_data$data = as.numeric(calculated_data$data)
```

```
calculated_data=calculated_data[!is.na(calculated_data$data),]
calculated_data$Date = as.Date(calculated_data$times, format = " %m/%d/%Y")
observed_data$Date = as.Date(observed_data$times, format = " %m/%d/%Y")
calculated_data=calculated_data[order(calculated_data$Date),]
observed_data=observed_data[order(observed_data$Date),]
calculated_data$times = factor(calculated_data$times, ordered = T)
calculated_data$times = factor(calculated_data$times, ordered = T)
longafter <- ggplot(data = observed_data,
                    aes(
                      x = Date,
                      y = data,
                      group = name,
                      fill = name
                    )) +
  geom_point(size = 4,
             stroke = 1.5,
             aes(color = name,
                 shape = name)) +
  geom_line(size = 1,
            data = calculated_data,
            aes(color = name,
                linetype = name)) +
  scale_shape_manual(values = c(16, 12), guide = "none") +
  scale_linetype_manual(values = c("solid", "twodash"), guide = "none") +
  scale_color_manual(values = c("#1F78B4", "#920000", "#1F78B4", "#920000"),
                     guide = "none") +
  scale_x_date(date_labels = "%Y/%m",
               date_breaks  = "3 month",
               name = "") +
  scale_y_continuous(breaks = round(seq(
    -1, 26, by = 5
  ), 2)) +
  ylab("d-excess (‰)") +
  theme_classic() +
  theme(axis.text.x = element_text(
    angle = 45,
    vjust = 1,
    hjust = 1
  ),
  axis.text = element_text(size = 16),
  axis.title = element_text(size = 18),
  legend.position = "none")
plot(y = beta_errors, x = betas, ylab = "RSME", xlab = "Beta values", main = "RSME of the
   different Beta values in 2017-21")
plot(y = taus_errors, x = taus, ylab = "RSME", xlab = "Tau values", main = "RSME of the different
   Tau values in 2017-21")
```

```
calculated_data_1_period$data
signs(calculated_data_1_period$data , accuracy = .0000001)
sequence =seq(-1, 26, by = 5)
sequence[1] = paste0("¥U2212", 1)
png(filename = "C:¥¥/Users/ /OneDrive/ / /", width = 2000, height = 1000, res = 300)
alldata_plot = ggplot(data = observed_data_1_period,
                      aes(
                        x = Date,
                        y = data,
                        group = name,
                        fill = name
                      )) +
  geom_point(size = 1,
             stroke = 0.7,
             aes(color = name,
                 shape = name)) +
  geom_line(#size = 1,
            data = calculated_data_1_period,
            aes(color = name,
                linetype = name)) +
  geom_point(size = 1,
             data = observed_data_2_period,
             stroke = 0.7,
             aes(color = name,
                 shape = name)) +
  geom_line(#size = 1,
            data = calculated_data_2_period,
            aes(color = name,
                linetype = name)) +
  geom_point(size = 1,
             data = observed_data_3_period,
             stroke = 0.7,
             aes(color = name,
                 shape = name)) +
  geom_line(#size = 1,
            data = calculated_data_3_period,
            aes(color = name,
                linetype = name)) +
  scale_shape_manual(values = c(16, 17), guide = "none") +
  scale_linetype_manual(values = c("solid", "twodash"), guide = "none") +
  scale_color_manual(values = c("#1F78B4", "#E69F00", "#1F78B4", "#E69F00"),
                     guide = "none") +
  scale_x_date(date_labels = "%Y/%m",
               date_breaks  = "6 month",
               name = "") +
  scale_y_continuous(breaks = round(seq(
```

```
    -1, 26, by = 5
  ), 2),
  labels=sequence
  ) +
  ylab("d-excess (‰)") +
  theme_classic() +
  theme(axis.text.x = element_text(
    angle = 45,
    vjust = 1,
    hjust = 1
  ),
  axis.text = element_text(size = 10),
  axis.title = element_text(size = 12),
  legend.position = "none")
print(alldata_plot)
dev.off()
tmp = calculated_data_1_period[,c(1,2,4)] %>% filter(name =="calculated_all")
write.csv(tmp,           file          =          "C:¥¥/Users/isbap/OneDrive/Área          de
   Trabalho/RCalculation_new/all_plots_all_2010_11.csv")
tmp = calculated_data_1_period[,c(1,2,4)] %>% filter(name =="calculated_out")
write.csv(tmp,           file          =          "C:¥¥/Users/isbap/OneDrive/Área          de
   Trabalho/RCalculation_new/all_plots_out_2010_11.csv")
tmp = calculated_data_2_period[,c(1,2,4)] %>% filter(name =="calculated_all")
write.csv(tmp,           file          =          "C:¥¥/Users/isbap/OneDrive/Área          de
   Trabalho/RCalculation_new/all_plots_all_2011_13.csv")
tmp = calculated_data_2_period[,c(1,2,4)] %>% filter(name =="calculated_out")
write.csv(tmp,           file          =          "C:¥¥/Users/isbap/OneDrive/Área          de
   Trabalho/RCalculation_new/all_plots_out_2011_13.csv")
tmp = calculated_data_3_period[,c(1,2,4)] %>% filter(name =="calculated_all")
write.csv(tmp,           file          =          "C:¥¥/Users/isbap/OneDrive/Área          de
   Trabalho/RCalculation_new/all_plots_all_2017_21.csv")
tmp = calculated_data_3_period[,c(1,2,4)] %>% filter(name =="calculated_out")
write.csv(tmp,           file          =          "C:¥¥/Users/isbap/OneDrive/Área          de
   Trabalho/RCalculation_new/all_plots_out_2017_21.csv")
filename_out = ('StreamWaterDexcessOutputLongAfterThinning2017-21.csv')
out_out1 = sapply(betas,
                  EPM,
                  tau = 39.11,
                  A = A_found,
                  filename = filename_out)
beta_errors = unlist(out_out1[1,])
out_out = sapply(taus,
                 EPM,
                 A = A_found,
                 beta = betas[which.min(beta_errors)],
                 filename = filename_out)
```

```
taus_errors = unlist(out_out[1,])
calculated_out = unlist(out_out[2,which.min(taus_errors)])
observed_out = unlist(out_out[3,1])
times_out = unlist(out_out[4,1])
tmp = data.frame(data = calculated_out, Date = times_out)
```